Resolving the physics of anisotropy, flow and chaotic fields

M. J. Hole[1], G. von Nessi[1], M. Fitzgerald[1], G. Dennis[1],
S. Hudson[2], R. L. Dewar[1], B. D. Blackwell[1],
J. Svensson[3], L. C. Appel[4]

[1] Australian National University, ACT 0200, Australia
[2] Princeton Plasma Physics Laboratory, New Jersey 08543, U.S.A.
[3] Max Planck Institute for Plasma Physics, Teilinstitut Greifswald, Germany
[4] EURATOM/CCFE Fusion Assoc., Culham Science Centre,Abingdon, Oxon OX14 3DB, UK

ITER

5th September 2012

Outline

- Motivation
- Australian fusion science research snapshot
- Anisotropy equilibrium and stability
  - Development of anisotropy into EFIT++
  - Determine impact of anisotropy on plasma stability
- Probabilistic (Bayesian) inference framework
  - Used to infer flux surface geometry with uncertainties
  - Provides model validation (equilibrium and mode structure)
  - Can be used to identify faulty diagnostics & optimise systems
  - Harnessed to infer properties of plasma (e.g. fast particle pressure)
- Multiple Relaxed Region MHD model
  - resolves chaotic field regions, islands, flux surfaces in fully 3D plasmas
  - Stepped Pressure Equilibrium Code.
  - Applied to DIIID RMP coils and ITER ELM coils as illustration.
- Summary

Australian Plasma Fusion Research Facility

- Australia's only fusion-relevant facility
- $30 million (ANU contribution ~$20 million)
- Facility funding extended to 2013.
  Infrastructure upgrade to
  - *Improve suitability as a testbed for ITER diagnostics*
  - *Improve plasma production/reliability/cleanliness*
  - *Improving opportunities for collaboration*
  - *Improve data analysis + provide computational support*
  - *Improve diagnostics*

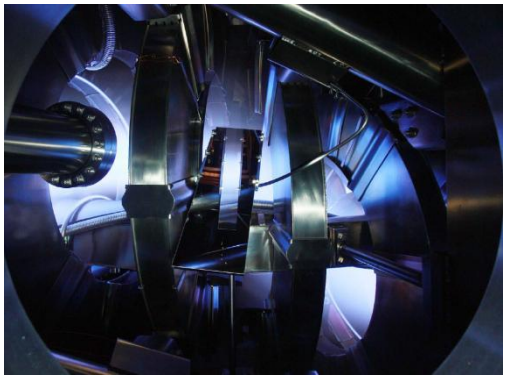

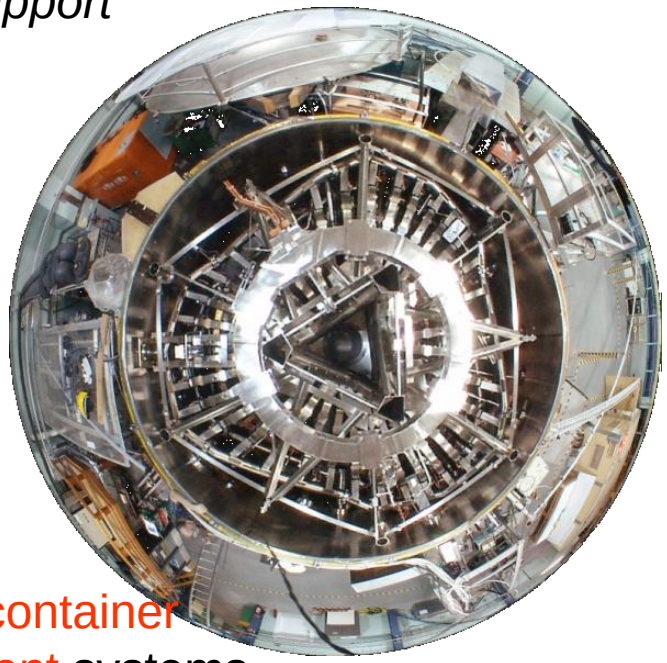

2011-12 Highlights:

- 2x200kW RF sources drive new phased antenna
- Third configuration control parameter added
- New Lab for materials diagnostics facility
- Upgraded impurity monitor system, interferometer
- Alfvén Excitation experiments

Mission:

- Study physics of hot plasma in a helical magnetic container
- Host development of advanced plasma measurement systems
- Contribute to global research, maintain Australian presence in fusion

Materials Diagnostic Test Facility Prototype

Mission:

- Resolve extreme plasma-surface interactions under controlled conditions (ANU + ANSTO + Univ. Syd. + Univ. Newcastle).
- Develop non-intrusive diagnostics for fusion relevant wall studies.

Initial results:

- B-dot probe indicates helicon wave propagation in argon.
- H plasma densities up to 10^{19} $m^{-3,}$ Argon ~2x higher
- Complex plasma flows observed by Dppler coherence imaging
- Exploratory W, C surface studies in H, He, Ar.a

Current status:

- Commissioned 20 kW pulsed RF power to provide P ~ 1MW m^{-2}
- Material target holder currently in production.

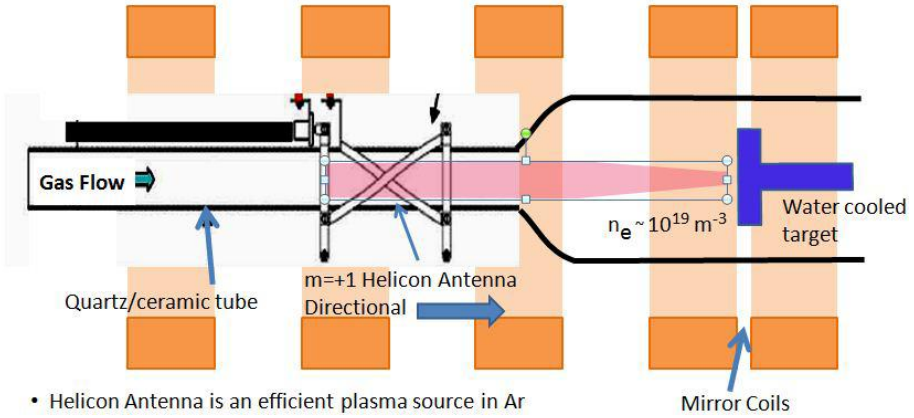

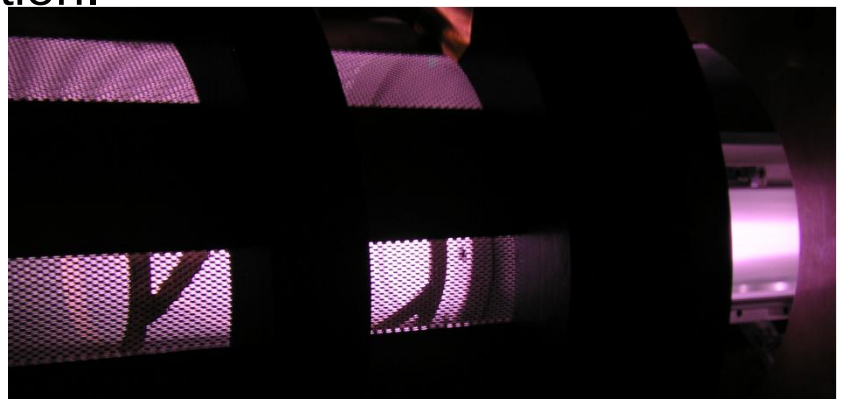

Australian Fusion Research Profile

- 3D MHD configuration physics:
  - Alfvén wave physics in fully 3D geometry
  - MRXMHD - partially relaxed MHD for fully 3D plasmas
- Diagnostics: Doppler imaging, MSE & CXRS imaging
- Plasma modelling, theory development
- Data mining: “clustering” fluctuation data across machines
- Bayesian integrated equilibrium modelling
- Plasma surface interaction studies
- Dust in plasmas
- Materials (e.g. MAX phase alloys), characterisation, modelling
- Atomic collision data physics

Very international. Some collaborators include ....

Outline

- Motivation
- Australian fusion science research snapshot
- Anisotropy equilibrium and stability
  - Development of anisotropy into EFIT++
  - Determine impact of anisotropy on plasma stability
- Probabilistic (Bayesian) inference framework
  - Used to infer flux surface geometry with uncertainties
  - Provides model validation (equilibrium and mode structure)
  - Can be used to identify faulty diagnostics & optimise systems
  - Harnessed to infer properties of plasma (e.g. fast particle pressure)
- Multiple Relaxed Region MHD model
  - resolves chaotic field regions, islands, flux surfaces in fully 3D plasmas
  - Stepped Pressure Equilibrium Code.
  - Applied to DIIID RMP coils and ITER ELM coils as illustration.
- Summary

Expected impact of anisotropy

- Small angle θ_b between beam, field $\Rightarrow p_{||} > p_{\perp}$
- Beam orthogonal to field, $\theta_b = \pi/2 \Rightarrow p_{\perp} > p_{||}$
- If $p_{||}$ sig. enhanced by beam, $p_{||}$ surfaces distorted and displaced inward relative to flux surfaces

  [Cooper et al, Nuc. Fus. 20(8), 1980]

- If $p\perp > p_{||}$, an increase will occur in centrifugal shift :

  [R. Iacono, A. Bondeson, F. Troyon, and R. Gruber, Phys. Fluids B 2 (8). August 1990]

- Compute $p_{\perp}$ and $p_{||}$ from moments of distribution function, computed by TRANSP

[M J Hole, G von Nessi, M Fitzgerald, K G McClements, J Svensson, PPCF 53 (2011) 074021]

- Infer $p_{\perp}$ from diamagnetic current $\mathbf{J}_{\perp}$

[see V. Pustovitov, PPCF 52 065001, 2010 and references therein]

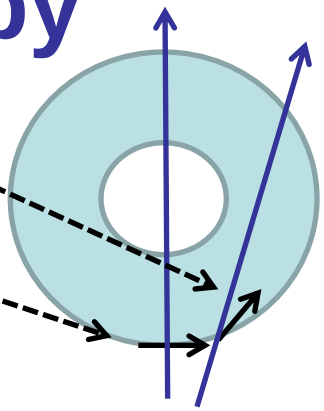

Peaked pressure profile

Broad pressure profile

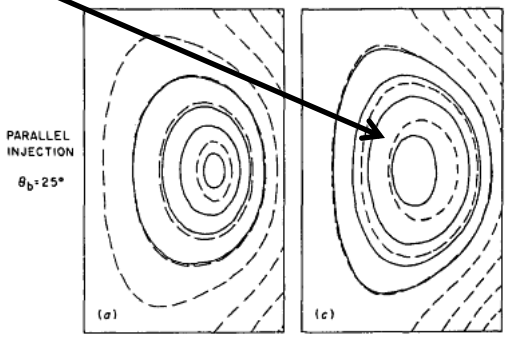

Parallel pressure contours(solid)

Flux surfaces (dashed)

Previous implementations of anisotropy

- Low-aspect-ratio , stationary
  W.A. COOPER et al NUCLEAR FUSION, Vol.20, No.8 (1980) 985

- EFIT, but no toroidal flow
  Zwingman, Eriksson and Stubberfield, Plasma Phys. Control. Fusion 43 (2001) 1441–1456

- FLOW, toroidal, poloidal flow and anisotropy, but not constrained to data
  L. Guazzotto, R. Betti, J. Manickam and S. Kaye, Phys. Plas. Vol. 11, 2004

- 3D anisotropic code ANIMEC
  W. A. Cooper, Comput. Phys. Commun. 180 (2009) 1524-1533.

- Why implement anisotropy into EFIT++?
  Contains many constraints to experimental data and iron/induction models.

MHD with rotation & anisotropy

- Inclusion of anisotropy and flow in equilibrium MHD equations

[R. Iacono, et al Phys. Fluids B 2 (8). 1990]

$$\nabla \cdot (\rho \mathbf{v}) = 0, \qquad \rho \mathbf{v} \cdot \nabla \mathbf{v} = \mathbf{J} \times \mathbf{B} - \nabla \cdot \bar{\mathbf{P}}, \qquad \nabla \cdot \mathbf{B} = 0$$

$$\mu_0 \mathbf{J} = \nabla \times \mathbf{B}, \qquad \nabla \times (\mathbf{v} \times \mathbf{B}) = 0,$$

$$\bar{\mathbf{P}} = p_\perp \bar{\mathbf{I}} + \Delta \mathbf{B}\mathbf{B}/\mu_0 , \qquad \Delta = \frac{\mu_0 (p_{||} - p_\perp)}{B^2}$$

MHD with rotation & anisotropy

- Inclusion of anisotropy and flow in equilibrium MHD equations

[R. Iacono, et al Phys. Fluids B 2 (8). 1990]

$$\nabla\cdot(\rho\mathbf{v})=0, \qquad \rho\mathbf{v}\cdot\nabla\mathbf{v}=\mathbf{J}\times\mathbf{B}-\nabla\cdot\bar{\mathbf{P}}, \qquad \nabla\cdot\mathbf{B}=0$$

$$\mu_0\mathbf{J}=\nabla\times\mathbf{B}, \qquad \nabla\times(\mathbf{v}\times\mathbf{B})=0,$$

$$\bar{\mathbf{P}}=p_\perp\bar{\mathbf{I}}+\Delta\mathbf{BB}/\mu_0\,, \qquad \Delta=\frac{\mu_0(p_{||}-p_\perp)}{B^2}$$

- Frozen flux gives velocity:

$$\mathbf{v}=\frac{\psi'_M(\psi)}{\rho}\mathbf{B}-R\phi'_E(\psi)\mathbf{e}_\varphi.$$

Equilibrium eqn becomes:

$$\nabla\cdot\left[\tau\left(\frac{\nabla\psi}{R^2}\right)\right]=-\frac{\partial p_\parallel}{\partial\psi}-\rho H'_M(\psi)+\rho\frac{\partial W}{\partial\psi}-I'_M(\psi)\frac{I}{R^2}-\psi''_M(\psi)\mathbf{v}\cdot\mathbf{B}+R\rho v_\phi\phi''_E(\psi)$$

$$I=RB_\varphi$$

$$I_M(\psi)=\tau\, I-\mu_0R^2\psi'_M(\psi)\phi'_E(\psi)$$

$$H_M(\psi)=W_M(\rho,B,\psi)-\frac{1}{2}[R\phi'_E(\psi)]^2+\frac{1}{2}\left[\frac{\psi'_M(\psi)B}{\rho}\right]^2,$$

$$\left\{I_M(\psi),\psi_M(\psi),\phi_E(\psi),H_M(\psi),\frac{\partial p_\parallel}{\partial\psi},\frac{\partial W}{\partial\psi}\right\}$$

Set of 6 profile constraints

$$\tau=1-\Delta-\mu_0(\psi'_M)^2/\rho,$$

Neglect poloidal flow

- Suppose $\mathbf{v} = -R\phi'_E(\psi)\mathbf{e}_\varphi = R\Omega(\psi)\mathbf{e}_\varphi \quad \Rightarrow \quad F(\psi) = I_M(\psi)/\tau$

and equilibrium eqn becomes:

$$\nabla\cdot\left[(1-\Delta)\left(\frac{\nabla\psi}{R^2}\right)\right] = -\frac{\partial p_\parallel}{\partial\psi} - \rho H'(\psi) + \rho\frac{\partial W}{\partial\psi} - \frac{F'(\psi)F'(\psi)}{R^2(1-\Delta)} + R^2\rho\Omega(\psi)\Omega'(\psi)$$

Set of 5 profile constraints

$$\left\{F(\psi), \Omega(\psi), H(\psi), \frac{\partial p_\parallel}{\partial\psi}, \frac{\partial W}{\partial\psi}\right\}$$

- $\partial W/\partial\psi$: different for MHD/ double-adiabatic/ guiding centre

- If two temperature Bi-Maxwellian model chosen

$$p_\parallel(\rho, B\psi) = \frac{k_B}{m}\rho T_\parallel(\psi) \qquad p_\perp(\rho, B\psi) = \frac{k_B}{m}\rho T_\perp(\psi) = \frac{k_B}{m}\rho T_\parallel(\psi)\frac{B}{B-\theta(\psi)T_\parallel}$$

$$\left\{F(\psi), \Omega(\psi), H(\psi), T_\parallel(\psi), \theta(\psi)\right\}$$

Implementation: EFIT++ overview

L. C. Appel

$$R^2\nabla\cdot\left(\frac{\nabla\psi}{R^2}\right)=-RJ_\phi(R,\psi)$$

$$J_\phi(R,\psi)=Rp'(\psi)+\frac{FF'(\psi)}{R}$$

$$p'(\psi)\approx\sum_i \hat{p}_i\bar{\psi}^i$$

$$FF'(\psi)\approx\sum_i \hat{F}_i\bar{\psi}^i$$

$\{p(\psi),F(\psi)\}$

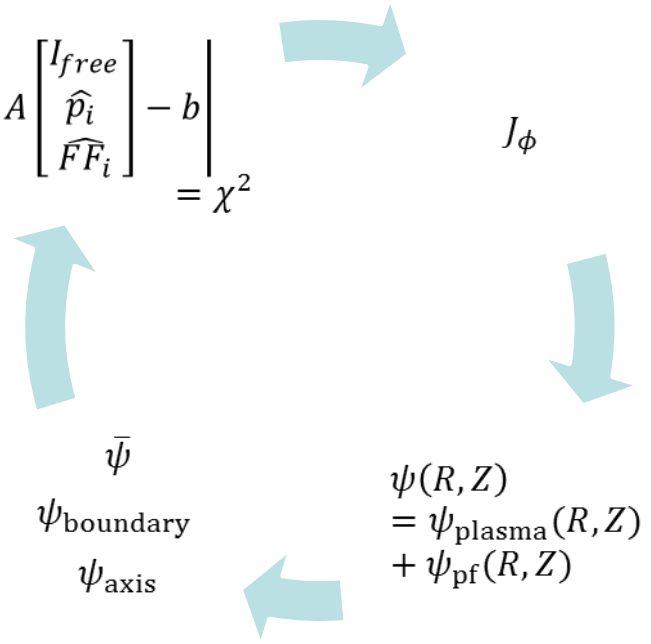

- Linear in plasma coefficients, linear least-squares eigenvalue problem, using response matrix A and measurements b (with errors)
- Compute plasma current J_ϕ
- Solve Grad-Shafranov equation for ψ
- Locate last closed flux surface and magnetic axis

EFIT++ (TENSOR) equations

M.Fitzgerald, L. C. Appel, M. J. Hole

$$\{F(\psi), \Omega(\psi), H(\psi), T_{\parallel}(\psi), \theta(\psi)\}$$

$$R^2 \nabla \cdot \left(\frac{\nabla \psi}{R^2}\right) = -R J_{\phi}(R,Z)$$

$$J_{\phi} = R\frac{k}{m}\rho T_{\parallel}'(\psi) + \frac{FF'(\psi)}{R(1-\Delta)} + \rho R^3 \Omega\Omega'(\psi) + R\rho H'(\psi) - R\rho\frac{\partial W}{\partial \psi} - R\nabla \cdot \left(\frac{\Delta}{R^2}\nabla\psi\right)$$

$$W(\rho, B, \psi) = \frac{k}{m} T_{\parallel} \ln\left(\frac{\rho}{\rho_0}\frac{|B - T_{\parallel}(\psi)\theta(\psi)|}{|B|}\right)$$

(Bi-Maxwellian)

$$\rho = \rho_0 \frac{T_{\perp}(\psi,B)}{T_{\parallel}(\psi)} \exp\left(\frac{mR^2\Omega^2(\psi)}{2kT_{\parallel}(\psi)}\right) \exp\left(\frac{mH(\psi)}{kT_{\parallel}(\psi)}\right)$$

$$T_{\parallel}'(\psi) \approx \sum_i \widehat{T}_i \overline{\psi}^i, FF'(\psi) \approx \sum_i \widehat{FF}_i \overline{\psi}^i,$$

$$\Omega\Omega'(\psi) \approx \sum_i \widehat{\Omega\Omega}_i \overline{\psi}^i, H'(\psi) \approx \sum_i \widehat{H}_i \overline{\psi}^i, \theta'(\psi) \approx \sum_i \widehat{\theta}_i \overline{\psi}^i$$

- Equations re-arranged into the form of a G-S equation with non-linear terms (red) expressed as a current.
- Current almost a linear combination of flux functions or flux functions times density.
- Shift of pressure profiles from magnetic surfaces caused by density.

Constraining the flux functions to transport codes or experiment

$$\{F(\psi), \Omega(\psi), H(\psi), T_{\|}(\psi), \theta(\psi)\}$$

- TRANSP computes *f(E,λ):* Moments give $p_{\perp}$, $p_{\|}$, $u_{\|}$,
- Dependency of flux functions on (R,Z) mesh

$$T_{\|}(R_i, Z_i) = \frac{p_{\|}(R_i,Z_i)}{\left(\frac{k}{m}\right)\rho(R_i,Z_i)}$$

$$F(R_i, Z_i) = R_i B_{\phi}(R_i, Z_i)[1 - \Delta(R_i, Z_i)]$$

$$\Omega(R_i, Z_i) = \frac{v_{\phi}(R_i,Z_i)}{R_i}$$

$$H(R_i, Z_i) = \frac{p_{\|}(R_i,Z_i)}{\rho(R_i,Z_i)} \ln\left(\frac{\rho(R_i,Z_i)p_{\|}(R_i,Z_i)}{\rho_0 p_{\perp}(R_i,Z_i)}\right) - \frac{v_{\phi}^2(R_i,Z_i)}{2}$$

$$\theta(R_i, Z_i) = \frac{\left(\frac{k}{m}\right)\rho(R_i,Z_i)B(R_i,Z_i)}{p_{\|}(R_i,Z_i)} - \frac{\left(\frac{k}{m}\right)\rho(R_i,Z_i)B(R_i,Z_i)}{p_{\perp}(R_i,Z_i)}$$

Code benchmarked

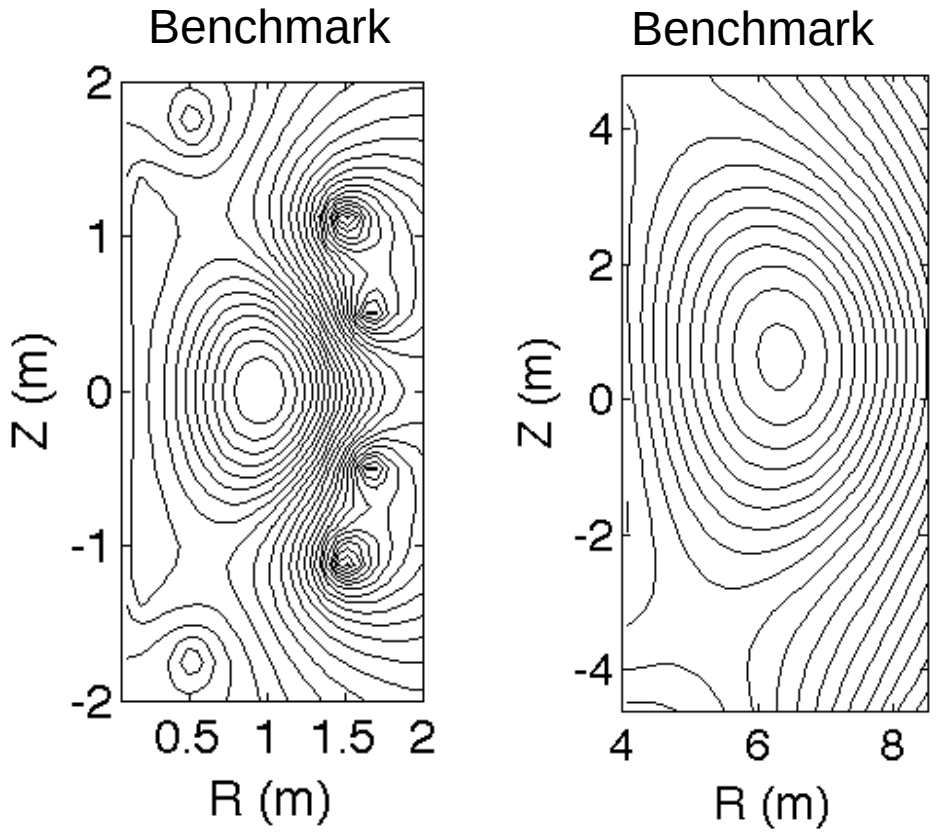

- So far tested (isotropic) against MAST #13050, #18696
- Able to use the same constraints as existing EFIT++
- Converges at same speed as existing EFIT++

Anisotropy on MAST

- MAST #18696
- 1.9MW NB heating
- I_p = 0.7MA, β_n=2.5
- TRANSP simulation available
- Magnetics shows CAEs

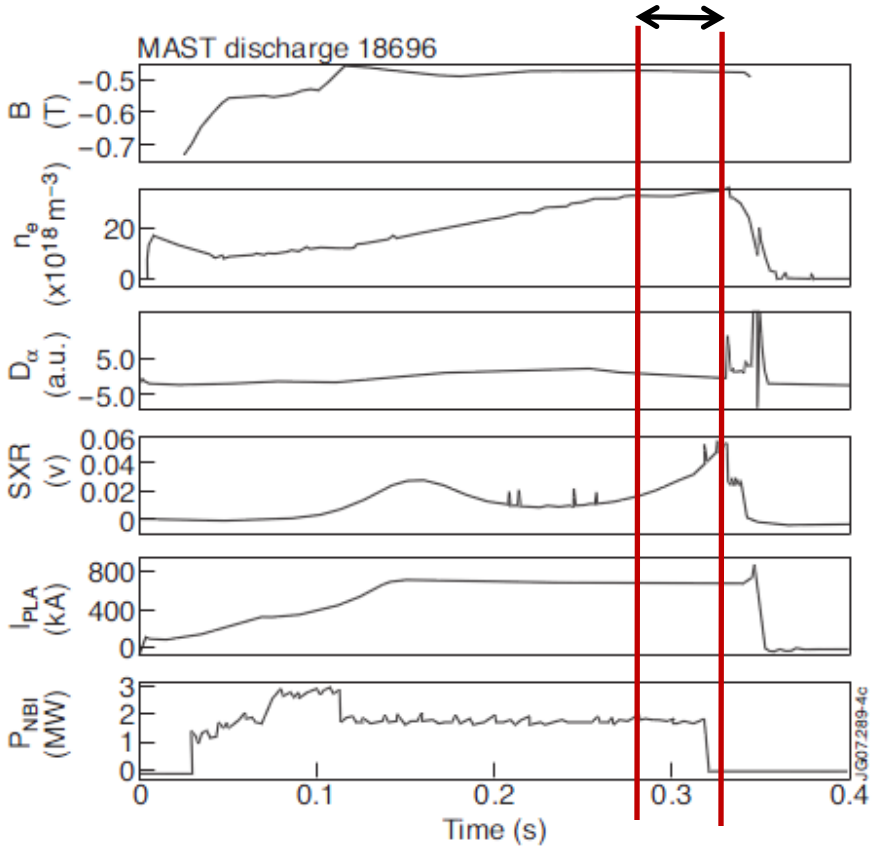

Magnetics

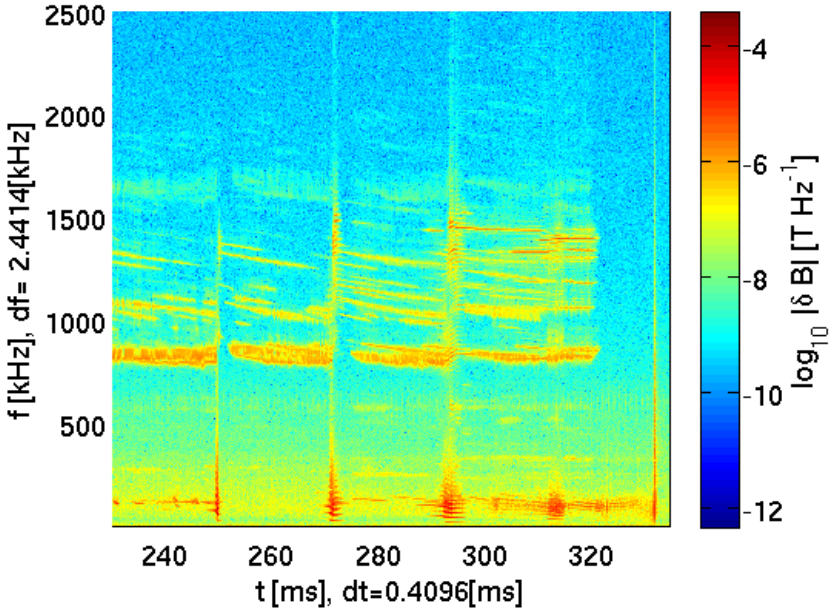

[M.P. Gryaznevich et al, Nuc. Fus. 48, 084003, 2008.; Lilley *et al* 35th EPS Conf. Plas.Phys. 9 - 13 June 2008 ECA Vol.32D, P-1.057]

- What is the impact on q profile due to presence of anisotropy and flow?

$p_{||}$, $p_{\perp}$, flow from $f(E,\lambda)$ moments

r/a=0.25

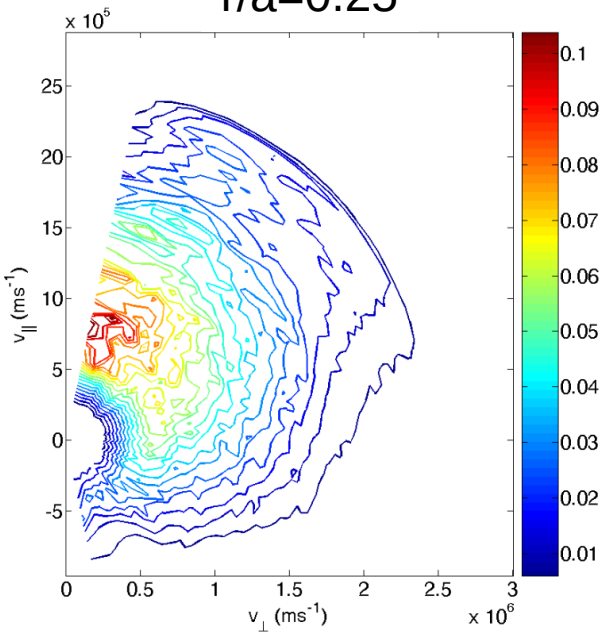

[35th EPS 2008; M.K.Lilley et al]

$$E = 0.5mv^2, \quad v_{\|} = v\cos\lambda$$

$$n = \int_0^{\infty}\int_{-1}^{1} \hat{f}(E,\lambda)\,\mathrm{d}\lambda\,\mathrm{d}E$$

$$nu_{\|} = \int_0^{\infty}\int_{-1}^{1} v_{\|}\hat{f}(E,\lambda)\,\mathrm{d}\lambda\,\mathrm{d}E$$

$$p_{\|} = m\int_0^{\infty}\int_{-1}^{1} (v_{\|}-u_{\|})^2\hat{f}(E,\lambda)\,\mathrm{d}\lambda\,\mathrm{d}E$$

$$p_{\perp} = \frac{m}{2}\int_0^{\infty}\int_{-1}^{1} v_{\perp}^2\hat{f}(E,\lambda)\,\mathrm{d}\lambda\,\mathrm{d}E.$$

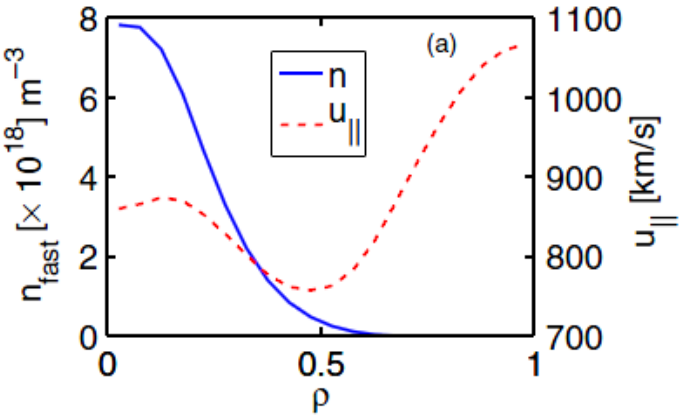

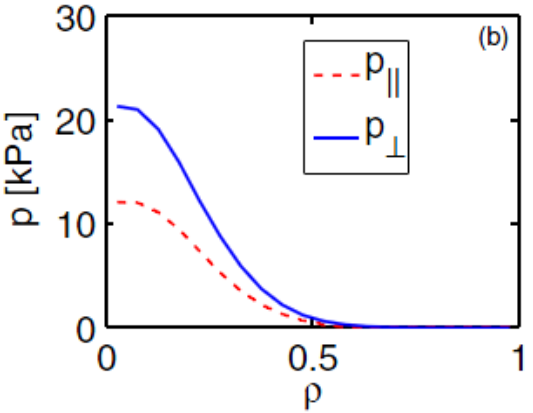

$p_{\perp}/p_{||} \approx 1.7$

$$\rho = \sqrt{\Phi/\Phi_0}$$

Φ = toroidal flux

[M J Hole, G von Nessi, M Fitzgerald, K G McClements and J Svensson, PPCF 53 (2011) 074021]

Impact of anisotropy on equilibrium

- Impact on configuration computed using FLOW

  [Guazzotto L, Betti R, Manickam J and Kaye S 2004 PoP11 604–14]

  $\Delta < 0$: $p_\perp / p_{||} \approx 1.7$ $\Delta = 0$: $p_\perp / p_{||} = 1$

Impact of anisotropy on equilibrium

- Impact on configuration computed using FLOW

  [Guazzotto L, Betti R, Manickam J and Kaye S 2004 PoP11 604–14]

  Δ <0: $p_\perp/p_{||} \approx 1.7$ Δ =0: $p_\perp/p_{||} = 1$ $\Delta = \mu_0 (p_\parallel - p_\perp)/B^2$
- Toroidal rotation does not change q appreciably with $M_{A,\varphi} \leq 0.3$
- Increase in q_0 ~ 100% for case with anisotropy

FLOW scans

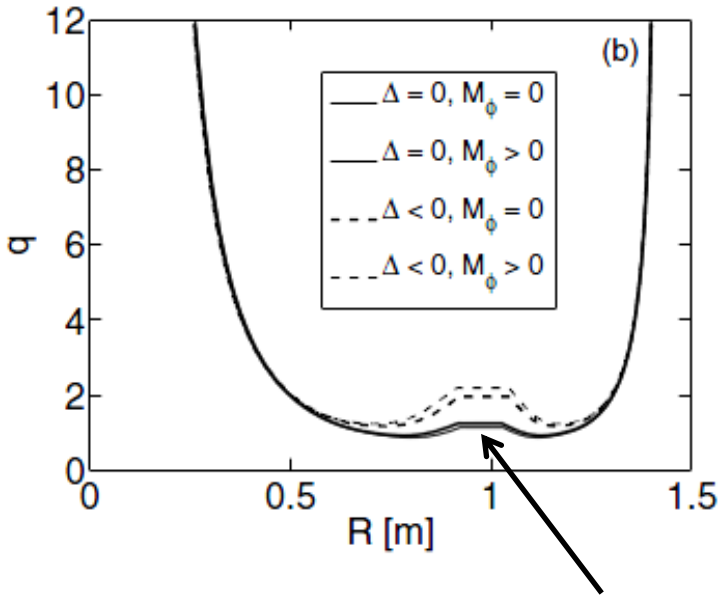

Low grid resolution of FLOW at core

EFIT++ (TENSOR)

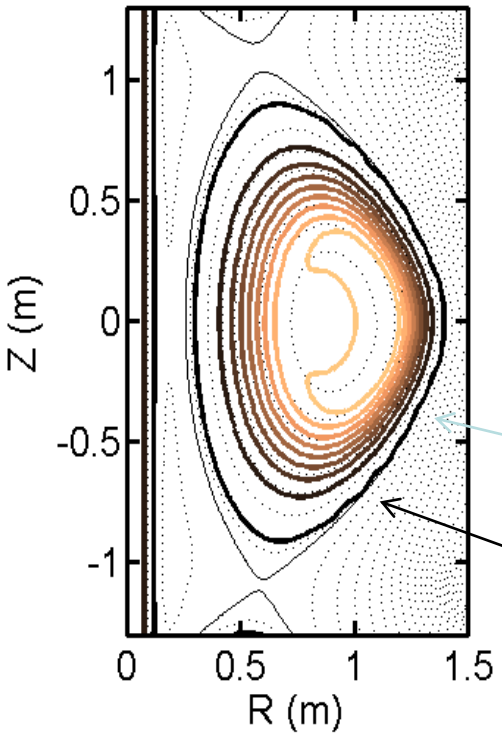

Calculation of MAST #18696 at 290ms.

$p_\perp / p_{||}$ ~ 1.7

poloidal flux

surfaces of constant $p_{||}$.

Impact of anisotropy on wave modes

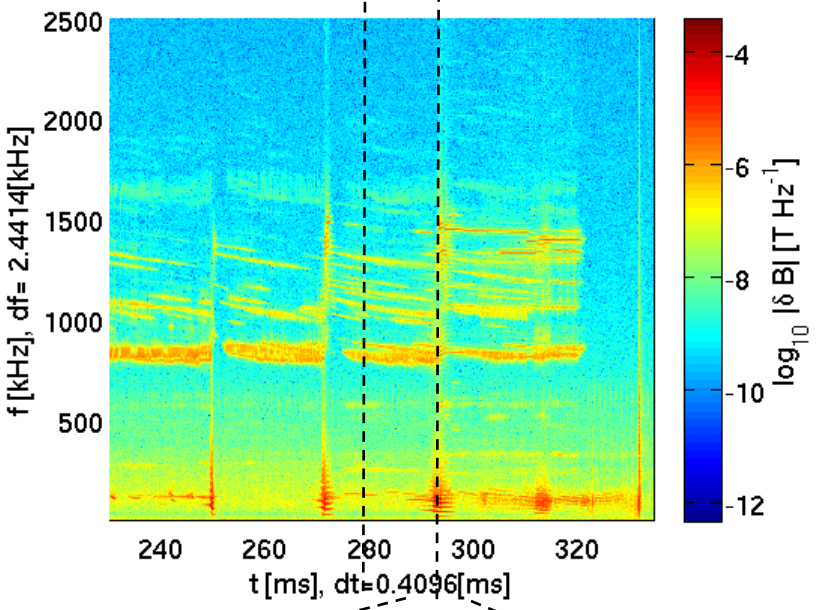

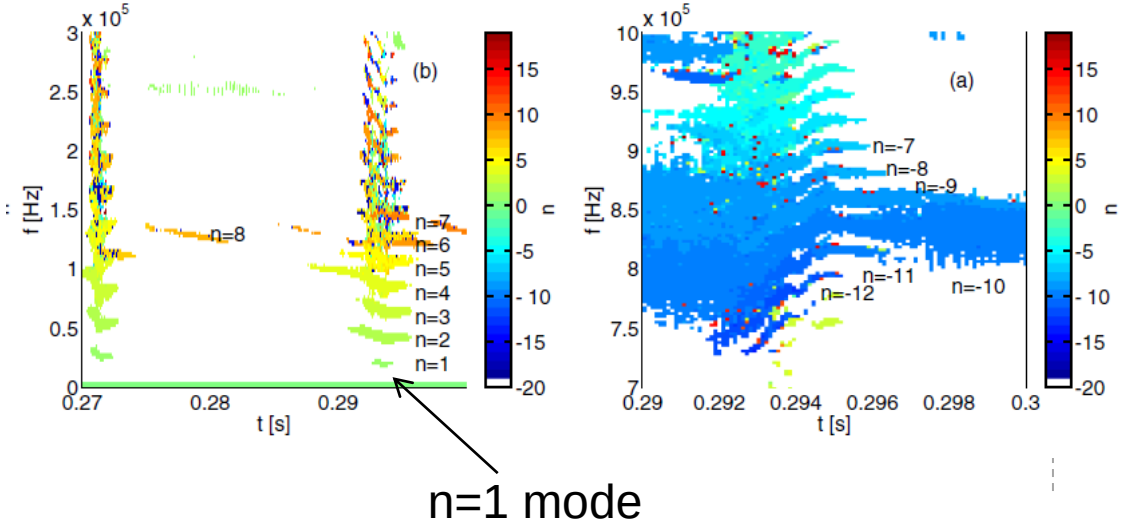

n=1 mode

- How do predicted mode frequencies change due to changes in *q* produced by anisotropy and flow?
- Calculation of change in stability due to anisotropy in progress.
- Appetiser: What is the change in ideal MHD stability of n=1 TAE and n=-10 CAE?

Increased shear gives multiple TAEs

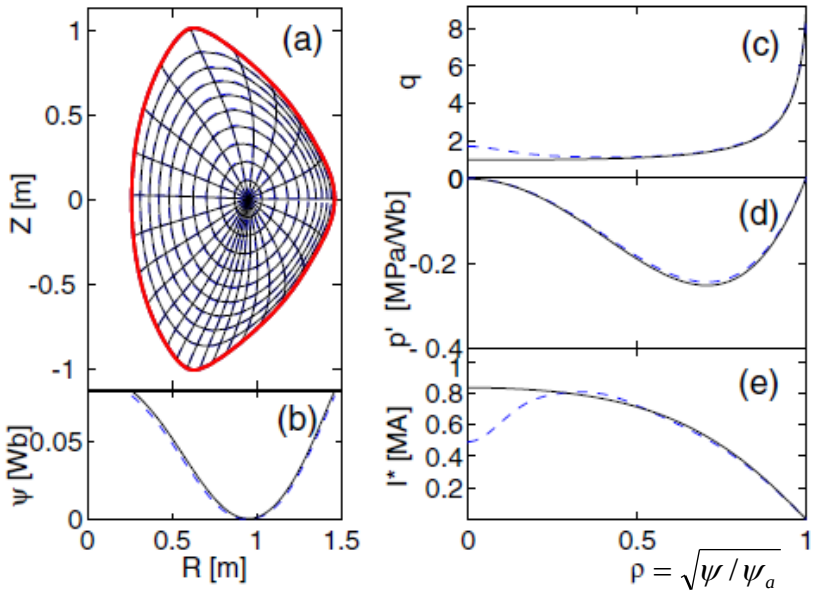

- Reshape plasma to have larger reverse shear

$$I^*(s) \rightarrow I^*(s) + \underbrace{I_0 \exp\left[-\frac{(s-s_0)^2}{2\sigma_0^2}\right]}_{\text{core}} + \underbrace{I_1 \exp\left[-\frac{(s-s_1)^2}{2\sigma_1^2}\right]}_{\text{reverse shear}}$$

I_0, I_1 varied to match q_0=1.7, q_{min}=1.24

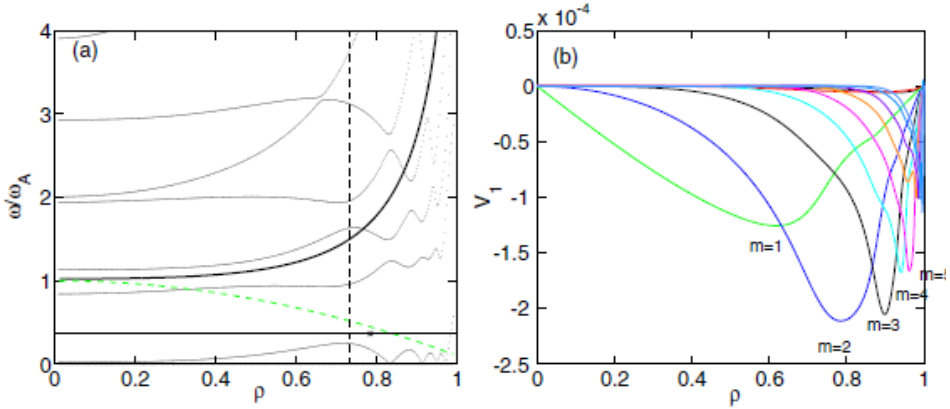

Single global TAE at (m,n) = (1,1)

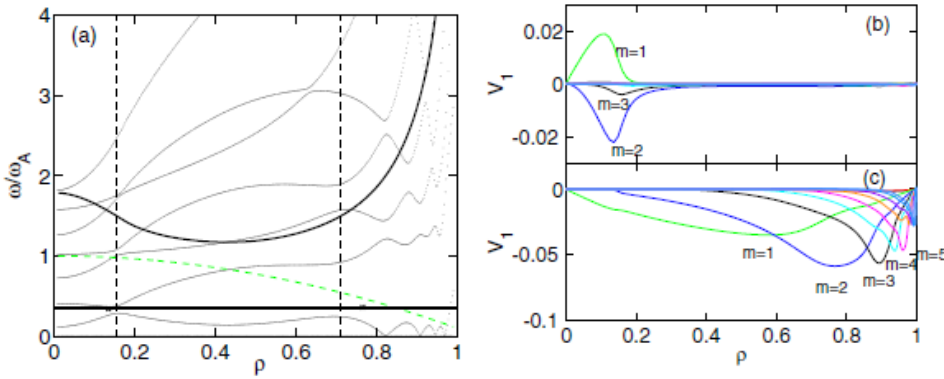

Reverse shear produces second (m,n)) = (1,1) odd TAE resonance in the core

CAE frequency: impact of change in q

CAE eigenfrequency [Smith et al PoP 10(5),1437-1442,2003]

$$\omega_{|n|,s,p} \simeq \frac{v_A}{\rho_0}\sqrt{\frac{n^2 q^2}{\kappa^2} + k_p + \frac{|n|q}{\kappa}\alpha_{sp}},$$

$$k_p = \left(1-\kappa^{-2}\right)\left(10p^2 - 2p + 3\right)/4$$

$$\alpha_{sp} = f_s\left(\rho_0 / R\right)\sqrt{1+\left(3+R_0/\rho_0\right)^2} + f_p\sqrt{1-R_0/\kappa^2 R}$$

Known: R_0= major radius, κ = ellipticity, n=-10
Inferred: p= poloidal mode no. = $|n|q_{mn}$
Unknown:
s= radial mode no. = 0 (guess)
ρ_0= radial localisation of mode ~ a/2 (guess)

Illustration

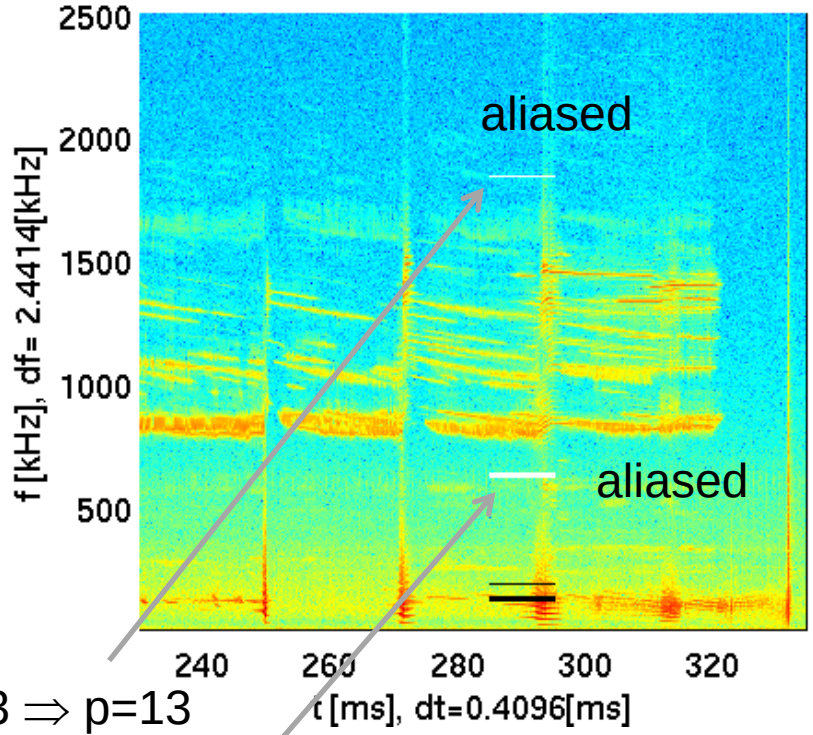

Static, isotropic equilibrium: $q_{mn}(R=R_0+a/2) = 1.3 \Rightarrow p=13$

Flowing, anisotropic equilibrium: $q_{mn}(R=R_0+a/2) = 1.3 \Rightarrow p=15$.

Anisotropy work in progress / planned

- Formulation of stability in presence of anisotropy, flow
- Implement anisotropy extensions of the global stability code MISHKA-F
- Couple the wave particle interaction code HAGIS to the TENSOR anisotropy module of EFIT++, and MISHKA-F
- Extend the Alfvén and ion sound wave continuum code CSCAS to include anisotropy.
- Use anisotropy inputs in ANIMEC to explore impact of anisotropy in 3D (no flow).

Outline

- Motivation
- Australian fusion science research snapshot
- Anisotropy equilibrium and stability
  - Development of anisotropy into EFIT++
  - Determine impact of anisotropy on plasma stability
- Probabilistic (Bayesian) inference framework
  - Used to infer flux surface geometry with uncertainties
  - Provides model validation (equilibrium and mode structure)
  - Can be used to identify faulty diagnostics & optimise systems
  - Harnessed to infer properties of plasma (e.g. fast particle pressure)
- Multiple Relaxed Region MHD model
  - resolves chaotic field regions, islands, flux surfaces in fully 3D plasmas
  - Stepped Pressure Equilibrium Code.
  - Applied to DIIID RMP coils and ITER ELM coils as illustration.
- Summary

Inference of energetic physics

Jakob Svensson, Gregory von Nessi, Lynton Appel,

ANU/CCFE/IPP developed a probabilistic framework based on Bayes' theorem for validating models for equil. & mode structure

Motivation:

- handle data from multiple diagnostics with strong model dependency
- provides a validation framework for different equilibrium models: e.g. Two fluid with rotation, multi-fluid, MHD with anisotropy
- yield uncertainties in inferred physics parameters (e.g. q profile) from models, data, and their uncertainties.
- Can be inverted : By reducing force-balance model uncertainty to zero, use as a technique to infer physics difficult to experimentally diagnose directly (e.g. Energetic particle pressure)

Bayesian equilibrium modelling

$$P(\mathbf{H}|\mathbf{D}) = P(\mathbf{D}|\mathbf{H})P(\mathbf{H}) / P(\mathbf{D})$$

$$\mathbf{H} = \left\{ J_\phi(R,Z),\ p'(\psi),\ f(\psi),\ \rho(\psi,R),\ \Omega(\psi) \right\}$$

$$\mathbf{D} = \left\{ P_i(R,Z),\ F_i(R,Z),\ \tan\ \gamma_i(R,Z),\ P_{s,e},\ S_e(k,\omega),\ S_C(\nu) \right\}$$

Pick-up coils	Flux loops	MSE signals	TS spectra	CXRS spectra

Aims

(1) Improve equilibrium reconstruction

(2) Validate different physics models

- Two fluid with rotation
  - [McClements & Thyagaraja Mon. Not. R. Astron. Soc. 323 733–42 2001]
- Ideal MHD fluid with rotation
  - [Guazzotto L et al, Phys. Plasmas 11 604–14, 2004]
- Energetic particle resolved multiple-fluid
  - [Hole & Dennis, PPCF 51 035014, 2009]

(3) Infer poorly diagnosed physics parameters

“Linear” current tomograhy

- Model the MAST plasma current as a cluster of rectangular, toroidal current beams that fill out the limiter region.
- Aim is to infer the distribution for each of these plasma beam currents (ie. **H** = vector of currents, I).
- Constraints:
  - Pick up coils data, P_i (**+**)
  - Flux loops data, F_i (*)
  - MSE data, tan γ_i

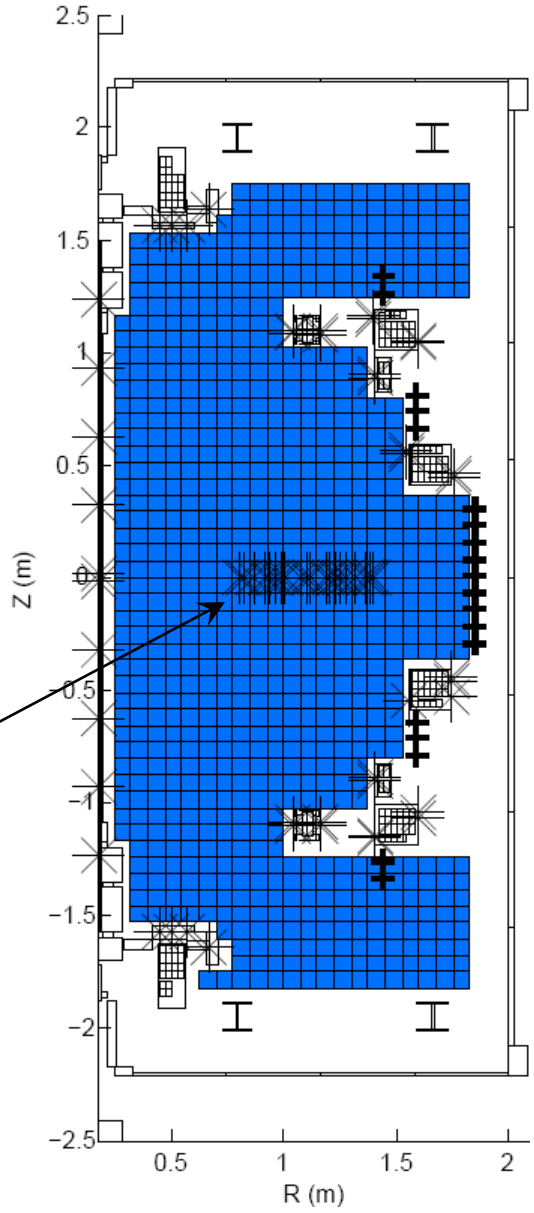

[Svensson J and Werner A *Plasma Phys. Control. Fusion* 50 085002 , 2008]

Forward models for magnetics and MSE

- Forward model describes predicted signal given plasma parameters (ie. **D|H** in P(**D|H**)). For pickup coils P_i, flux loops F_i and polarisation angle γ_i

Angle between coil normal and midplane

$$P_i(R,Z;I) = B_R(R,Z;I)\cos(\theta_i) + B_Z(R,Z;I)\sin(\theta_i)$$

$$F_i(R,Z;I) = \psi(R,Z;I)$$

$$\tan\gamma_i(R,Z;I) = \frac{A_0 B_Z(R,Z;I) + A_1 B_R(R,Z;I) + \cancel{A_2 B_\phi(R,Z;I)}}{\cancel{A_3 B_Z(R,Z;I) + A_4 B_R(R,Z;I)} + A_5 B_\phi(R,Z;I)}$$

- MSE viewing optics on midplane $\Rightarrow A_2 = A_3 = A_4 \approx 0$.
- If B_ϕ taken as vacuum field, P_i, F_i, $\tan\gamma_i$ are linear in I. Hence:

$$\mathbf{P} = \mathbf{M}\mathbf{I} + \mathbf{C}$$

prediction — response — current

Mean in posterior gives flux surfaces

- If current beams *I* have a Gaussian pdf ⇒ inference analytic

- MAST #24600 @280ms
- D plasma, 3MW NB heating
- I_p = 0.8MA, β_n=3

Current Tomography

Poloidal flux surfaces

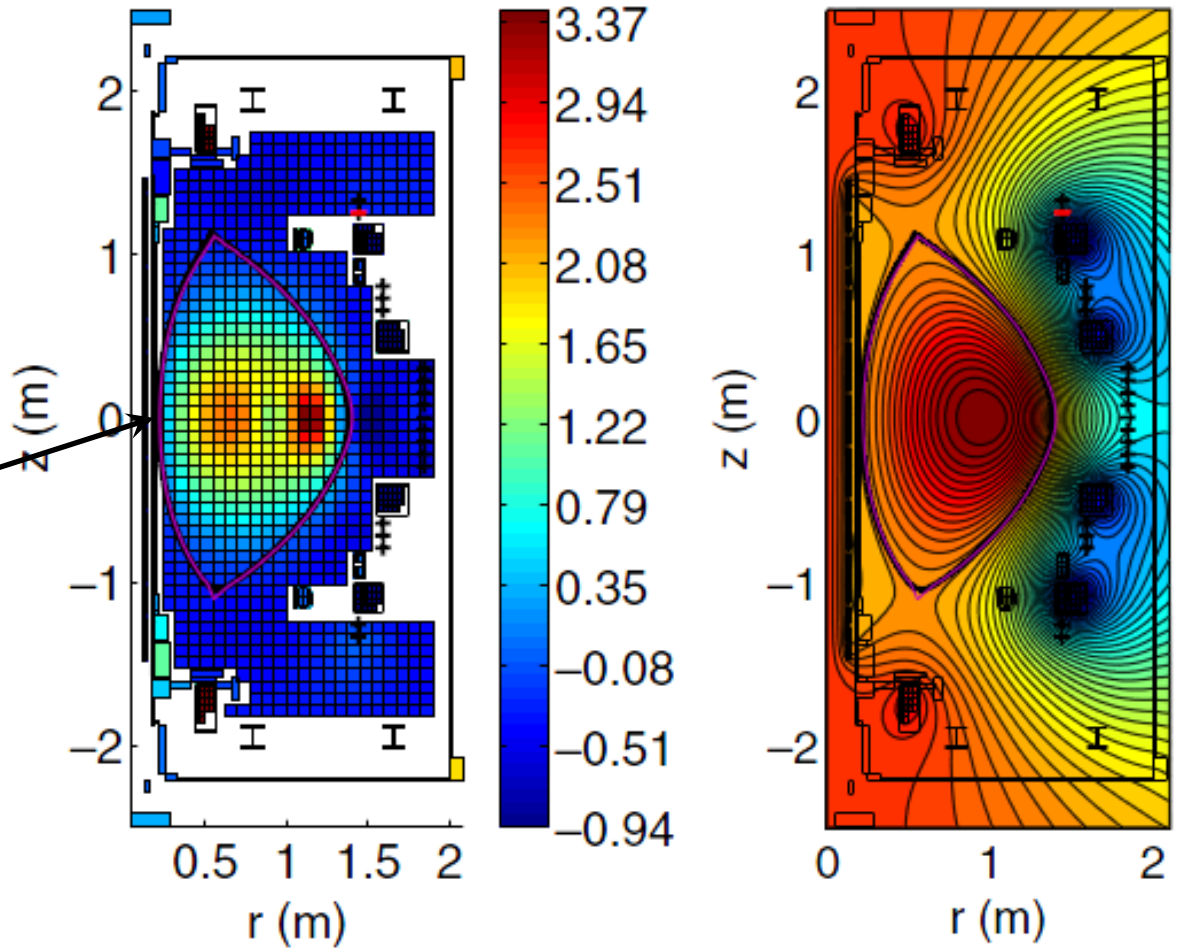

Last closed flux surface of MSE& EFIT

J_ϕ and ψ surfaces plotted for currents corresponding to the maximum of the posterior

[M.J. Hole, G. von Nessi, J. Svensson, L.C. Appel, Nucl. Fusion 51 (2011) 103005]

Sampling of posterior gives distribution

- Distributions generated by sampling, e.g. q profile

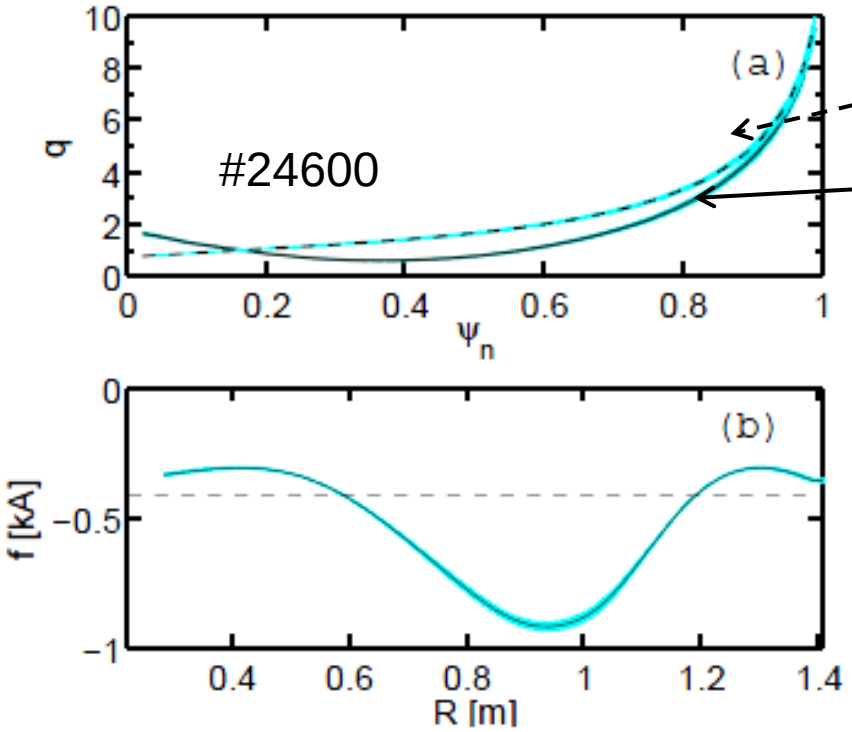

No poloidal currents

Inference of poloidal currents: allow f(ψ) to be a 4th-order polynomial in ψ

Errors < 5%, but are model dependant

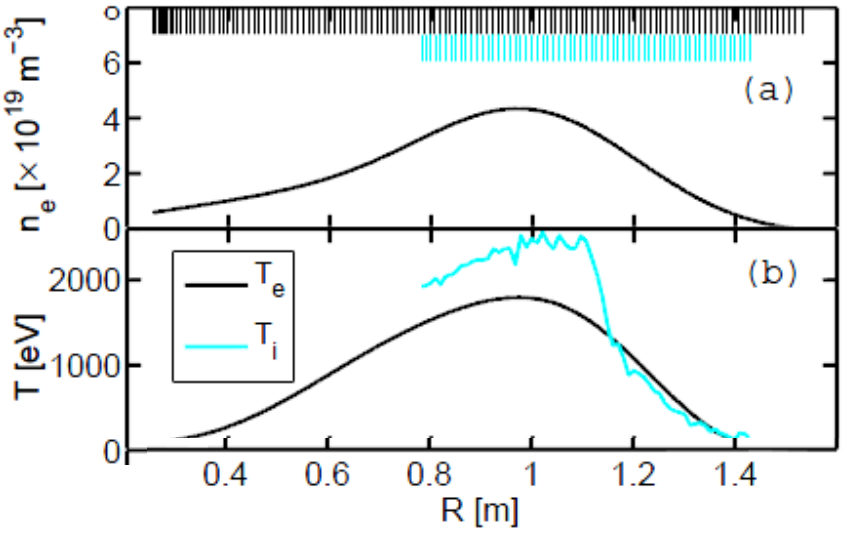

- Bayesian models for TS and CXRS

Bayesian **E**quilibrium **A**nalysis & **S**imulation **T**ool

Gregory von Nessi

- Fold in Force balance model as a weak constraint by technique of split observations.
- Allows quantification of agreement of force-balance through evidence

Biot-Savart link to diagnostics

$$-\frac{R}{2\pi\mu_0}\nabla\cdot\left[\left(\frac{\nabla\psi}{R^2}\right)\right] = J_\phi = -2\pi R p'(\psi) + \frac{\mu_0}{2\pi R} f(\psi) f'(\psi)$$

$$P(\mathbf{H}|\mathbf{D}) = \frac{P(\mathbf{D}|\mathbf{H})P(\mathbf{H})}{P(\mathbf{D})} = \frac{P_{1/2}(\mathbf{D}|\mathbf{H}_L)P_{1/2}(\mathbf{D}|\mathbf{H}_R)P(\mathbf{H})}{C_{1/2}P(\mathbf{D})}$$

- Grad-Shafranov equation is non-analytic
- Computationally challenges overcome by nested sampling.

Validation of force balance

Gregory von Nessi

MAST #22254 @ 350ms

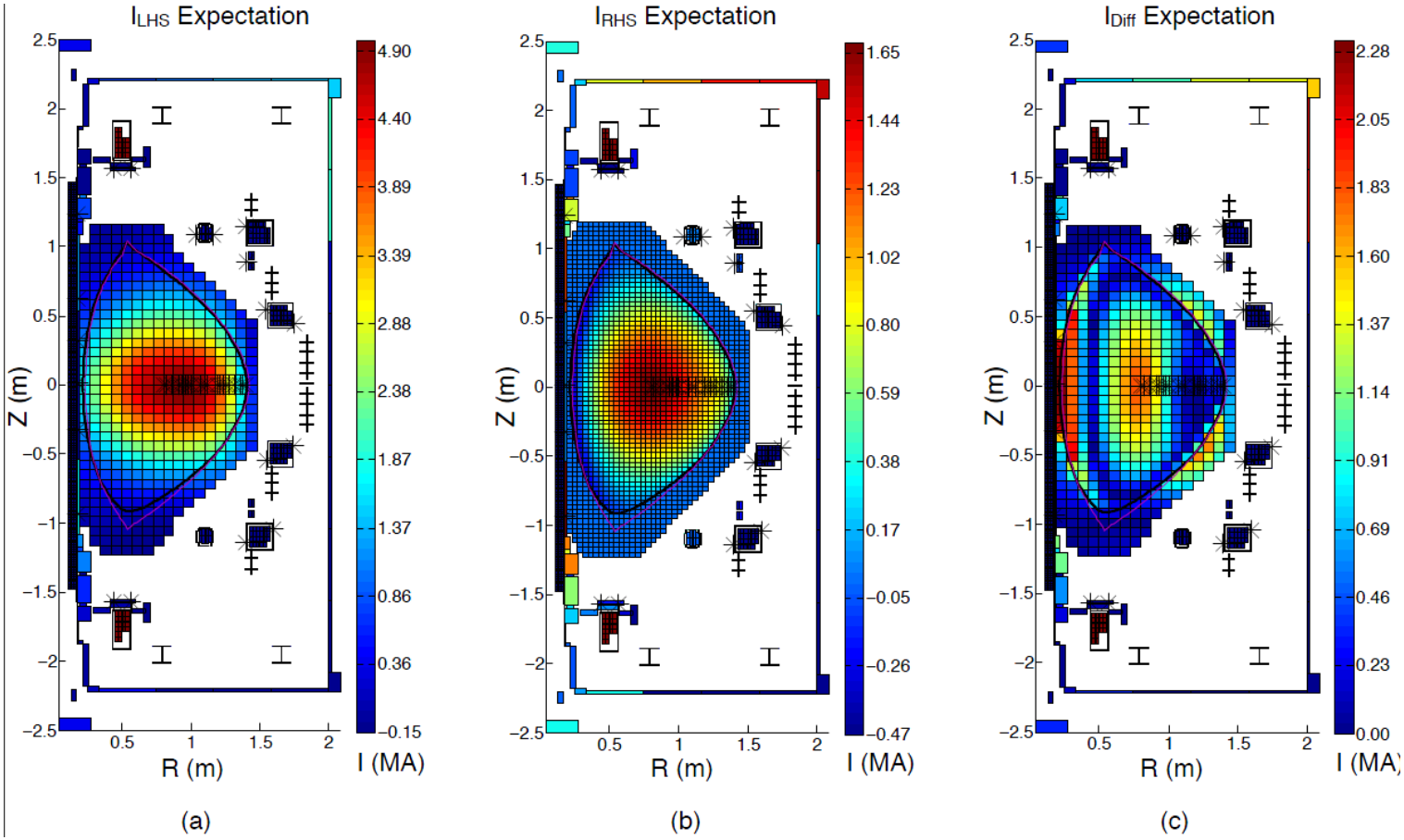

- Discrepancy between LHS & RHS ⇒ model not consistent with observations
- Agreement quantified by evidence ln(P(D))=1263.5
- Relative evidence between different models important

Energetic pressure inference

- add polynomial parameterisations of P_{total}, P_{therm} to *H*, and add analysed Thomson scattering data to *D*
- Assume
  $P_{therm} = (n_i T_i + n_e T_e) \sim n_e T_e$
  $f(\psi) \alpha \psi$
- Add a force-balance constraint $\Rightarrow$

$$P_{fast} = P_{tot} - P_{therm}$$

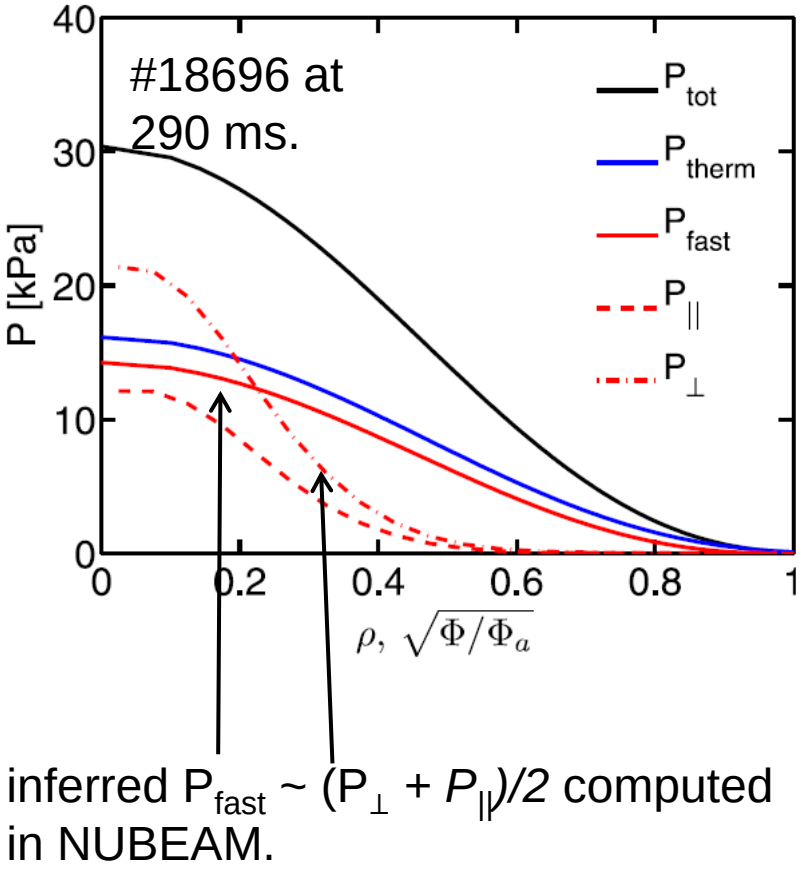

inferred $P_{fast} \sim (P_{\perp} + P_{||})/2$ computed in NUBEAM.

[M. J. Hole, G von Nessi, M Fitzgerald and the MAST team, Plasma Phys. Control. Fusion 54 (2012), accepted]

Evidence-based cross-validation:

Gregory von Nessi

...a systematic technique to identify faulty diagnostics.

- Identifies inconsistent diagnostics by maximising evidence.

[G. T. von Nessi, M. J. Hole, J. Svensson, and L. Appel Phys. Plasmas 19, 012506 (2012)]

1 A baseline posterior, P_0, is calculated with all diagnostics

2. One diagnostic observation, o_i, is removed, a new posterior P_i and log-evidence $E_i = \ln(P(D))$ computed. Repeat for all diagnostics.

3. The diagnostic with lowest E_i is removed, and a new baseline posterior calculated. The evidence of this new posterior is recorded and associated with the removed diagnostic.

4. Steps (1)–(3) repeated to generate a curve of posterior evidence versus the number of diagnostics removed.

5. Diagnostics removed such that the posterior evidence recorded in Step (3) is maximised.

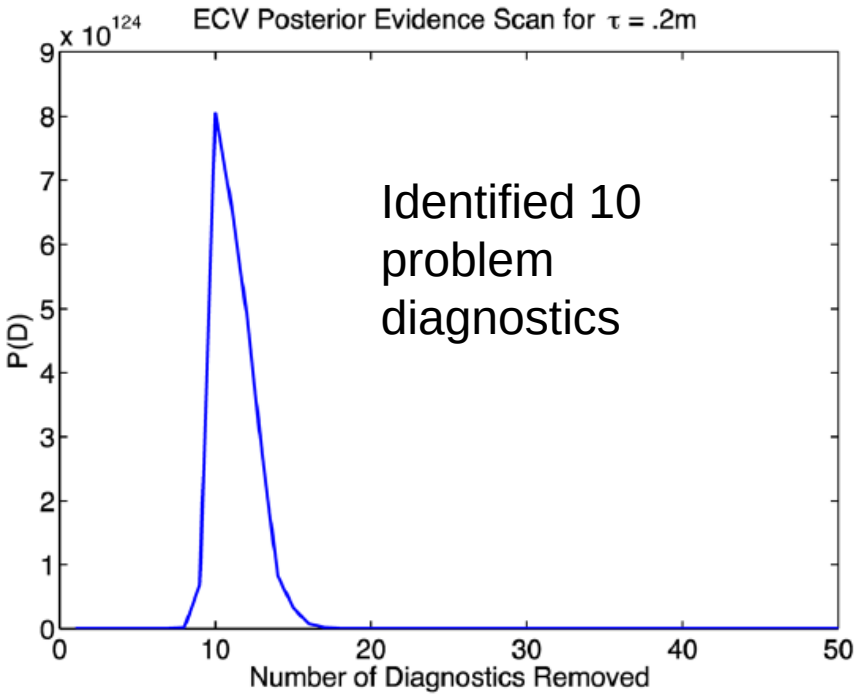

Outline

- Motivation
- Australian fusion science research snapshot
- Anisotropy equilibrium and stability
  - Development of anisotropy into EFIT++
  - Determine impact of anisotropy on plasma stability
- Probabilistic (Bayesian) inference framework
  - Used to infer flux surface geometry with uncertainties
  - Provides model validation (equilibrium and mode structure)
  - Can be used to identify faulty diagnostics & optimise systems
  - Harnessed to infer properties of plasma (e.g. fast particle pressure)
- Multiple Relaxed Region MHD model
  - resolves chaotic field regions, islands, flux surfaces in fully 3D plasmas
  - Stepped Pressure Equilibrium Code.
  - Applied to DIIID RMP coils and ITER ELM coils as illustration.
- Summary

Toroidal plasma equilibrium in 3D

- simplest model to approximate global, macroscopic force-balance in toroidal plasma confinement with arbitrary geometry is magnetohydrodynamics (MHD).

$$\nabla p = \mathbf{J} \times \mathbf{B}, \qquad \nabla \times \mathbf{B} = \mathbf{J}, \qquad \nabla \cdot \mathbf{B} = 0$$

- Non-axisymmetric magnetic fields generally **do not** have a nested family of smooth flux surfaces, **unless** ideal surface currents are allowed at the rational surfaces.

- If the field is non-integrable (i.e. chaotic, with a fractal phase space), then any **continuous** pressure that satisfies $\mathbf{B}\cdot\nabla p=0$ must have an **infinitely discontinuous gradient,** ∇p.

- Instead, solutions with stepped-pressure profiles are guaranteed to exist. A partially-relaxed, topologically-constrained, MHD energy principle is described.

- A numerical solver, SPEC (written by S. Hudson, PPPL), solves for these fields: field has islands, chaotic regions, and flux surfaces

Taylor Relaxed States

- Zero pressure gradient regions are **force-free** magnetic fields:

- In 1974, Taylor argued that turbulent plasmas with small resistivity, and viscosity relax to a Beltrami field

Internal energy: $$W = \int_{P \cup V} \left(\frac{B^2}{2\mu_0} + \frac{p}{\gamma - 1} \right) d\tau^3$$

Total Helicity : $$H = \int_V (\mathbf{A} \cdot \mathbf{B}) d\tau^3$$

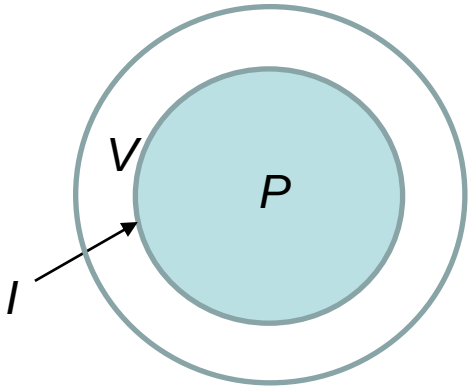

Taylor solved for minimum *W* subject to fixed *H*

i.e. solutions to δF=0 of functional $F = W - \mu H \ / 2$

$$P: \quad \nabla \times \mathbf{B} = \mu \mathbf{B}$$

$$I: \quad \left[\left[\frac{B^2}{2\mu_0} + p \right]\right] = 0$$

$$V: \quad \nabla \times \mathbf{B} = 0$$

Model had a lot of success for toroidal pinches, multipinch, and spheromaks

Generalised Taylor Relaxation:
Multiple Relaxed Region MHD (MRXMHD)

R. L. Dewar

- Assume each invariant tori I_i act as ideal MHD barriers to relaxation, so that Taylor constraints are localized to subregions.

New system comprises:

- N plasma regions P_i in relaxed states.
- Regions separated by ideal MHD barrier I_i.
- Enclosed by a vacuum V,
- Encased in a perfectly conducting wall W

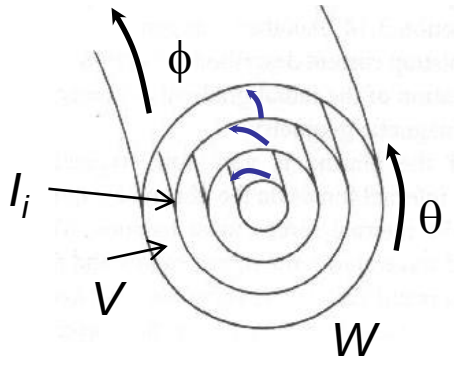

$$W_l = \int_{R_i} \left(\frac{B_l^{\,2}}{2\mu_0} + \frac{P_l}{\gamma - 1} \right) d\tau^3$$

$$H_l = \int_V (\mathbf{A}_l \cdot \mathbf{B}_l) d\tau^3$$

Seek minimum energy state:

$$F = \sum_{l=1}^{N} \left(W_l - \mu_l H_l / 2 \right)$$

$$P_l: \quad \nabla \times \mathbf{B} = \mu_l \mathbf{B}$$

$$P_l = \text{constant}$$

$$I_l: \quad \mathbf{B} \cdot \mathbf{n} = 0$$

$$[[P_l + B^2/(2\mu_0)]] = 0$$

$$V: \quad \nabla \times \mathbf{B} = 0$$

$$\nabla \cdot \mathbf{B} = 0$$

$$W: \quad \mathbf{B} \cdot \mathbf{n} = 0$$

Existence of Three-Dimensional Toroidal MHD Equilibria with Nonconstant Pressure

OSCAR P. BRUNO
California Institute of Technology

PETER LAURENCE
Universita di Roma "La Sapienza"

We establish an existence result for the three-dimensional MHD equations

$$(\nabla \times \mathbf{B}) \times \mathbf{B} = \nabla p$$
$$\nabla \cdot \mathbf{B} = 0$$
$$\mathbf{B} \cdot n|_{\partial T} = 0$$

with $p \neq$ const in tori T *without symmetry*. More precisely, our theorems insure the existence of sharp boundary solutions for tori whose departure from axisymmetry is sufficiently small; they allow for solutions to be constructed with an arbitrary number of pressure jumps.

Communications on Pure and Applied Mathematics, Vol. XLIX, 717–764 (1996)

→ this was a strong motivation for pursuing the stepped-pressure equilibrium model

→ how large the "sufficiently small" departure from axisymmetry can be needs to be explored numerically

Stepped Pressure Equilibrium Code, SPEC

[Plasma Physics and Controlled Fusion, 54:014005, 2012] S. Hudson

Vector potential is discretised using mixed Fourier & finite elements

- Coordinates (s,φ, ζ)
- Interface geometry $R_i = \sum_{l,m,n} R_{lmn} \cos(m\vartheta - n\zeta),\ Z_i = \sum_{l,m,n} Z_{lmn} \sin(m\vartheta - n\zeta)$
- Exploit gauge freedom $\mathbf{A} = A_\vartheta(s,\vartheta,\zeta)\nabla\vartheta + A_\zeta(s,\vartheta,\zeta)\nabla\zeta$
- Fourier $A_\vartheta = \sum_{m,n} \alpha(s)\cos(m\vartheta - n\varsigma)$
- Finite-element $a_\vartheta(s) = \sum_i a_{\vartheta,i}(s)\varphi(s)$

& inserted into constrained-energy functional $F = \sum_{l=1}^{N} (W_l - \mu_l H_l / 2)$

- Derivatives wrt **A** give Beltrami field $\nabla \times \mathbf{B} = \mu\mathbf{B}$
- Field in each annulus computed independently, distributed across multiple cpu's
- Field in each annulus depends on enclosed toroidal flux, poloidal flux, interfaces ξ

Force balance solved using multi-dimensional Newton method

- Interface geometry adjusted to satisfy force balance $\mathbf{F}[\xi] = \{[\![p + B^2/2]\!]_{m,n}\} = 0$
- Angle freedom constrained by spectral condensation,
- Dertivative matrix ∇F[ξ] computed in parallel using finite difference

Numerical error scales as expected

Scaling of numerical error with radial resolution.

$\mathbf{A}=A_\vartheta \nabla\vartheta + A_\zeta \nabla\zeta$, $\mathbf{B}=\nabla\times\mathbf{A}$, $\mathbf{j}=\nabla\times\mathbf{B}$, need to quantify **error** = $\mathbf{j} - \mu\mathbf{B}$

$A_\vartheta, A_\zeta \sim O(h^n)$

h = radial grid size = 1 / N
n = order of polynomial

$$\sqrt{g}B^s = \partial_\vartheta A_\zeta - \partial_\zeta A_\vartheta \sim O(h^n)$$
$$\sqrt{g}B^\vartheta = -\partial_s A_\zeta \sim O(h^{n-1})$$
$$\sqrt{g}B^\zeta = \partial_s A_\vartheta \sim O(h^{n-1})$$

$$\sqrt{g}\,j^s \sim O(h^{n-1})$$
$$\sqrt{g}\,j^\vartheta \sim O(h^{n-2})$$
$$\sqrt{g}\,j^\zeta \sim O(h^{n-2})$$

$(j-\mu B)\cdot\nabla s \sim O(h^{n-1})$ $(j-\mu B)\cdot\nabla\theta \sim O(h^{n-1})$ $(j-\mu B)\cdot\nabla\zeta \sim O(h^{n-1})$

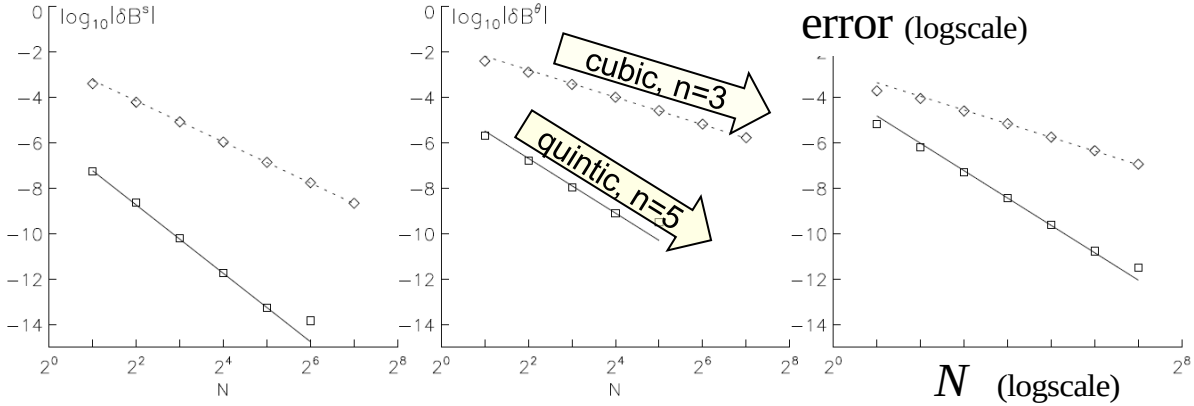

Example of chaotic Beltrami field in single given annulus;

$R = 1.0 + r(\vartheta,\zeta)\cos\vartheta,$
$Z = \quad r(\vartheta,\zeta)\sin\vartheta,$

inner surface
$r = 0.1$
outer interface
$r = 0.2 \; + \delta\left[\cos(2\vartheta-\zeta)+\cos(3\vartheta-\zeta)\right]$

(m,n)=(3,1) island + (m,n)=(2,1) island = chaos

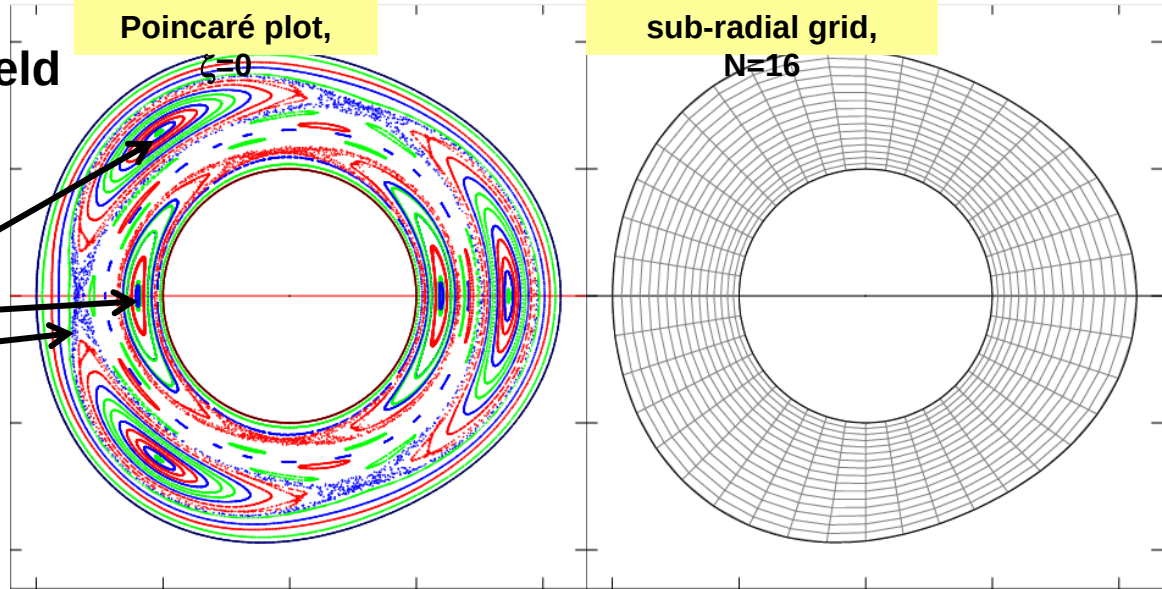

Example : DIIID with n=3 applied error field

- Axis-symmetric boundary, pressure profile from EFIT reconstruction, $\beta \approx 15\%$

Acknowledgement: Ed Lazarus, Sam Lazerson

- Apply 3mm, n=3 boundary deformation, (m=2,3,4)
- Strong pressure gradient near edge
- Irrational interfaces chosen to coincide with pressure gradients.

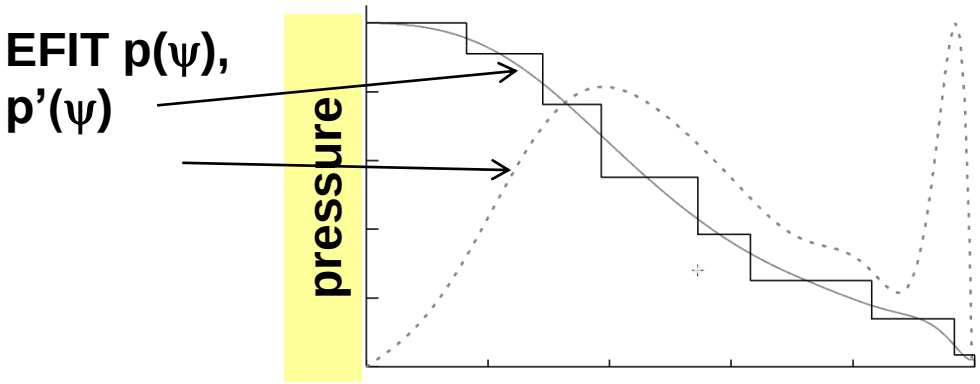

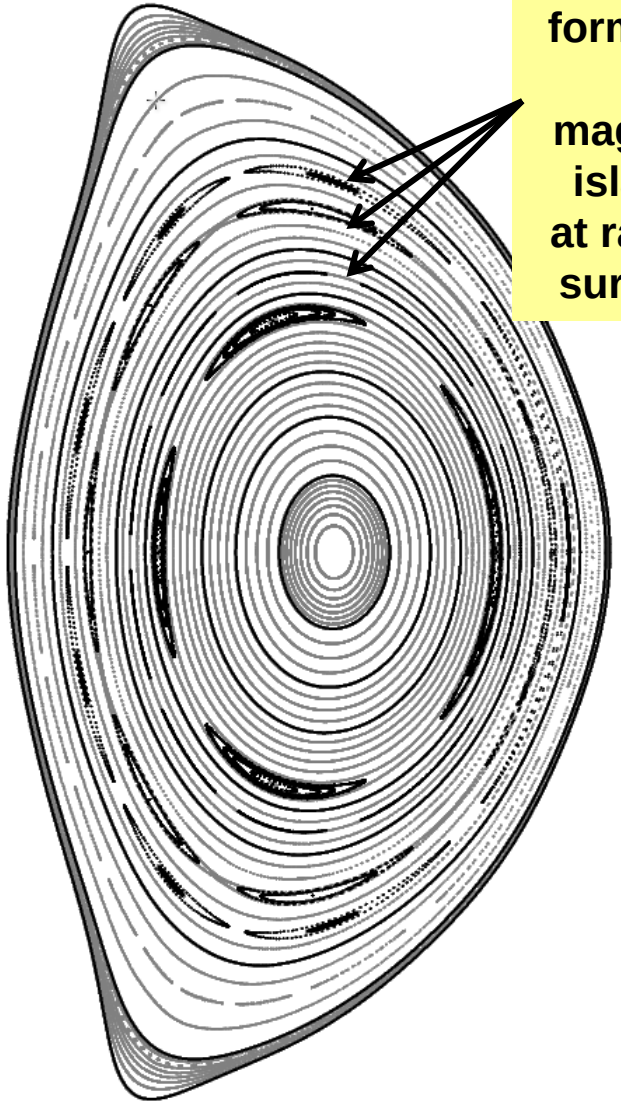

- Island formation is permitted
- No rational "shielding currents" included in calculation.

Example of ITER relevant configuration, with and without rational shielding currents

- If ideal constraint applied at rational surfaces, shielding currents prevent islands

ITER boundary, plus $\delta=10^{-4}$ perturbation.

$$\delta R = \delta \cos(2\vartheta - \phi)\cos\vartheta,$$
$$\delta Z = \delta \cos(2\vartheta - \phi)\sin\vartheta$$

rotational transform

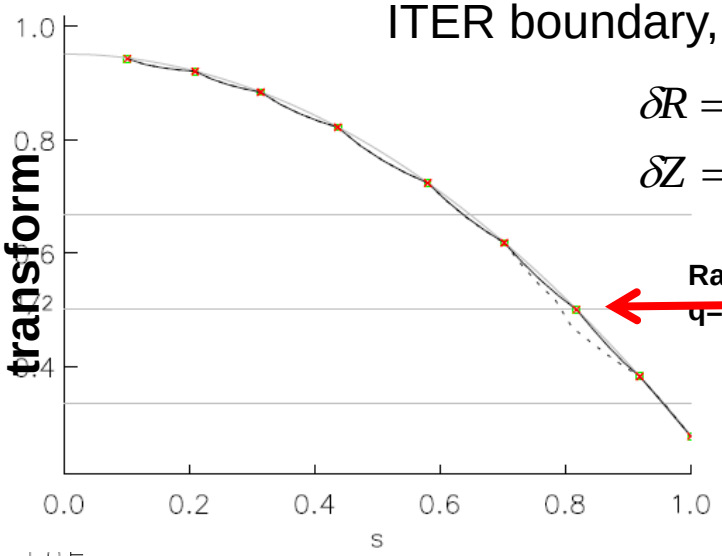

Rational surface q=2/1

pressure

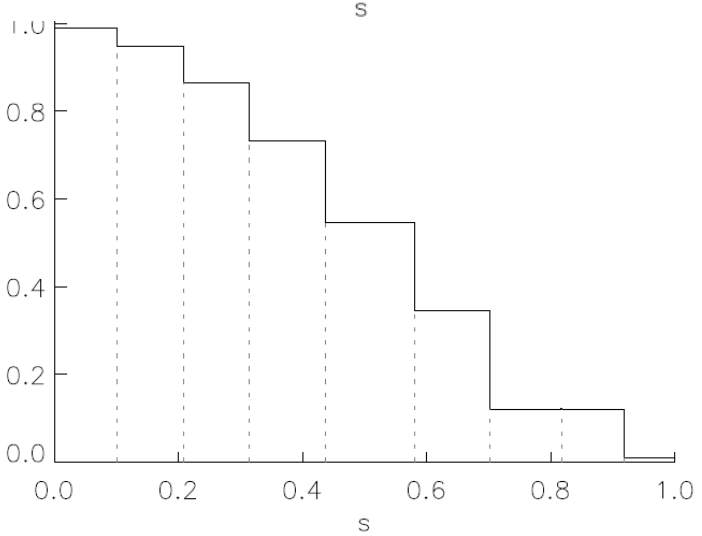

WITH rational ideal interface

no island formation

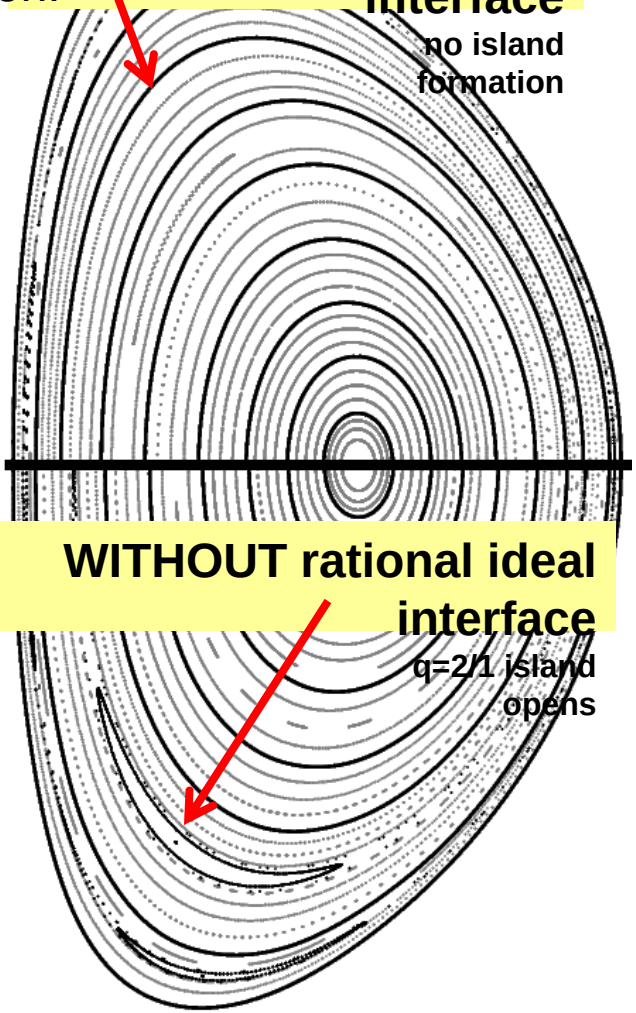

WITHOUT rational ideal interface

q=2/1 island opens

Spontaneous formed helical states

G. Dennis

- The quasi-single helicity state is a a stable helical state in RFP: becomes purer as current is increase

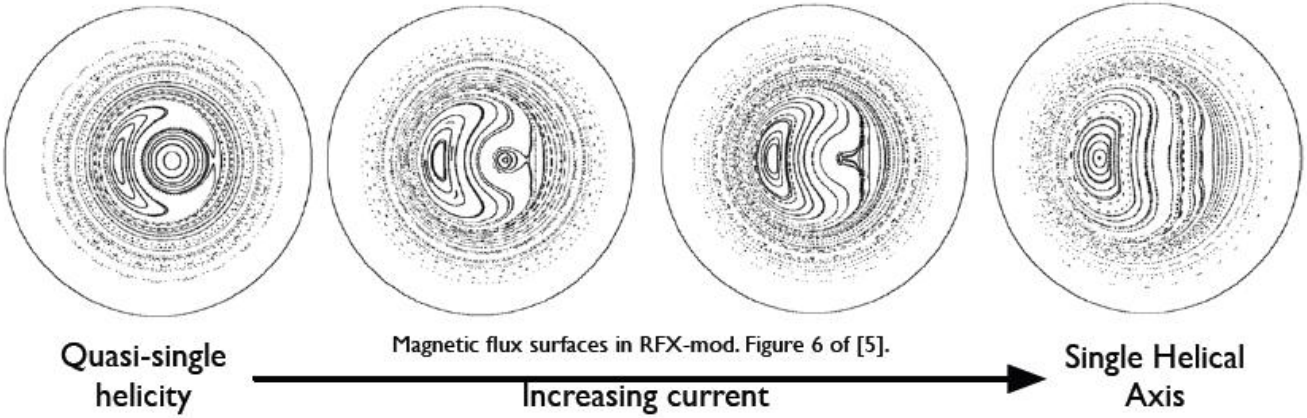

Magnetic flux surfaces in RFX-mod. Figure 6 of [5].

Fig. 6 of P. Martin *et al., Nuclear Fusion* ***49, 104019 (2009)***

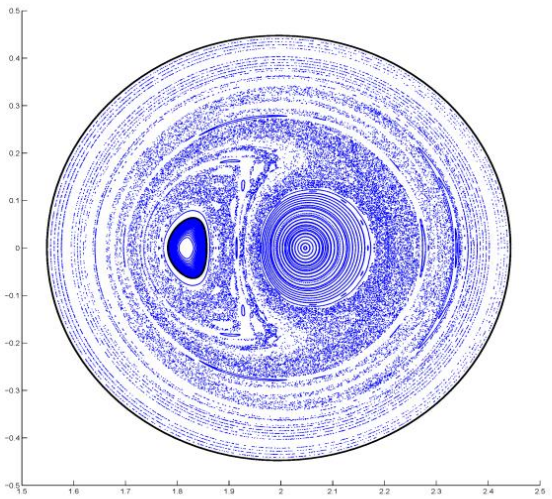

- Attempt to describe RFX-mod QSH state by a two-interface minimum energy MRXMHD state
- Calculation of the RFP bifurcated state, with energy lower than the comparable axis-symmetric state
- Both magnetic axes can be reproduced in addition to island structure and significant amounts of chaos

Summary

- Anisotropy equilibrium and stability
  - Development of anisotropy into EFIT++
  - Determine impact of anisotropy on plasma stability
- Bayesian validation framework for equilibrium
  - Provides q profile and uncertainty.
  - Motivation: validate equilibrium models
  - Exploited force balance discrepancy to infer P_{energ}
  - tools to optimally place diagnostics, identify faulty diagnostics
- Multiple Relaxed Region MHD model
  - resolves chaotic field regions, islands, flux surfaces in 3D plasmas
  - Stepped Pressure Equilibrium Code.
  - Applied to DIIID RMP coils and ITER ELM coils as illustration.
- *Strong interest in ITER physics. Opportunity to shape work to be more ITER relevant. Seek research participation through collaboration and competitive grants*

Stepped Pressure Equilibrium Code, SPEC

[Plasma Physics and Controlled Fusion, 54:014005, 2012] S. Hudson

Vector potential is discretised using mixed Fourier & finite elements

* toroidal coordinates (s,ϑ,ζ), *interface geometry $\mathrm{R}_l = \sum_{m,n} R_{l,m,n}\cos(m\vartheta - n\zeta), Z_l = \sum_{m,n} Z_{l,m,n}\sin(m\vartheta - n\zeta)$

* exploit gauge freedom $\mathbf{A} = A_\vartheta(s,\vartheta,\zeta)\nabla\vartheta + A_\zeta(s,\vartheta,\zeta)\nabla\zeta$

* Fourier $A_\vartheta = \sum_{m,n} a_\vartheta(s)\cos(m\vartheta - n\zeta)$

* Finite-element $a_\vartheta(s) = \sum_i a_{\vartheta,i}(s)\varphi(s)$

& inserted into constrained-energy functional $F = \sum_{l=1}^{N}\left(W_l - \mu_l H_l/2\right)$

* derivatives w.r.t. vector-potential → Beltrami field $\nabla\times\mathbf{B} = \mu\mathbf{B}$
* field in each annulus computed independently, distributed across multiple cpus
* field in each annulus depends on enclosed toroidal flux (boundary condition) and
  → poloidal flux, ψ_P, and helicity,
  → geometry of interfaces, $\boldsymbol{\xi} \equiv \left\{R_{m,n}, Z_{m,n}\right\}$

Force balance solved using multi-dimensional Newton method

* interface geometry is adjusted to satisfy force $\mathbf{F[\xi]} \equiv \left\{[[\mathrm{p}+B^2/2]]_{m,n}\right\}=0$
* angle freedom constrained by spectral-condensation, adjust angle freedom to minimize $\sum(m^2+n^2)\left(R_{mn}^2 + Z_{mn}^2\right)$
* derivative matrix, $\nabla\mathbf{F[\xi]}$, computed in parallel using finite-differences
* call NAG routine: quadratic-convergence w.r.t. Newton iterations; robust convex-gradient method;

Equilibria with (i) perturbed boundary & chaotic fields, and (ii) pressure are computed .

Poincaré plot (cylindrical)
β = 0%

Poincaré plot (cylindrical)
β ≈ 4%

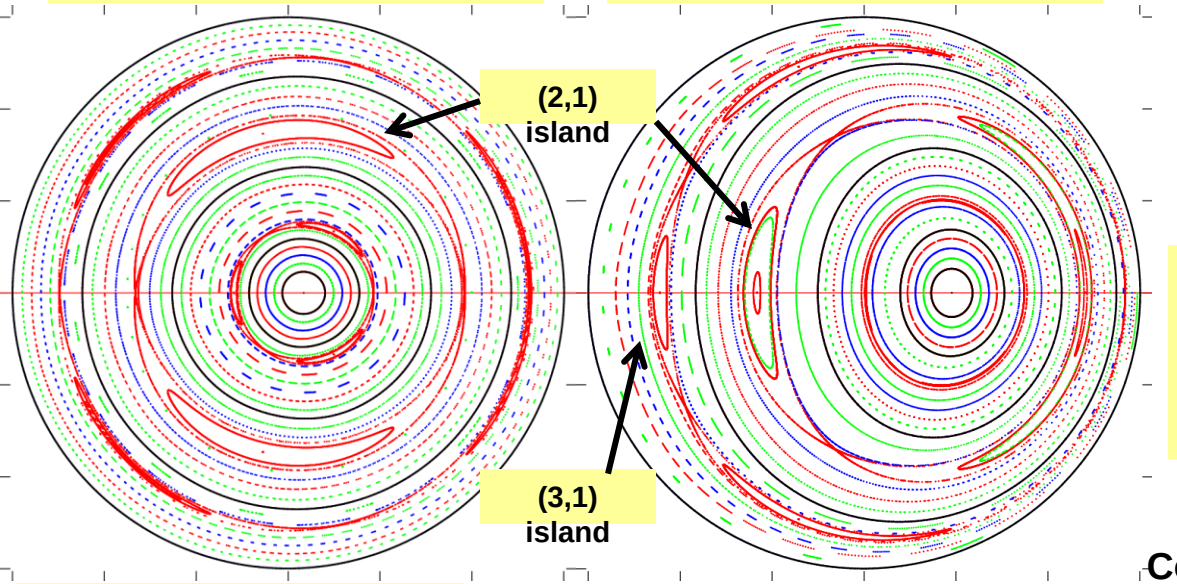

boundary deformation induces islands

$$R = 1.0 + r\cos\vartheta,\ Z = r\sin\vartheta$$

$$r = 0.3 + \delta\cos(2\vartheta - \phi) + \delta\cos(3\vartheta - \phi)$$

$$\delta = 10^{-4}$$

Demonstrated Convergence

of high-pressure equilibrium with islands,

with Fourier Resolution,

Convergence of (2,1) & (3,1) island widths

Poincaré plot (toroidal)
β ≈ 4%

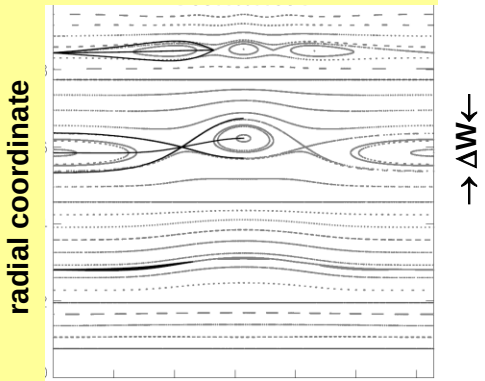

→ ΔW←

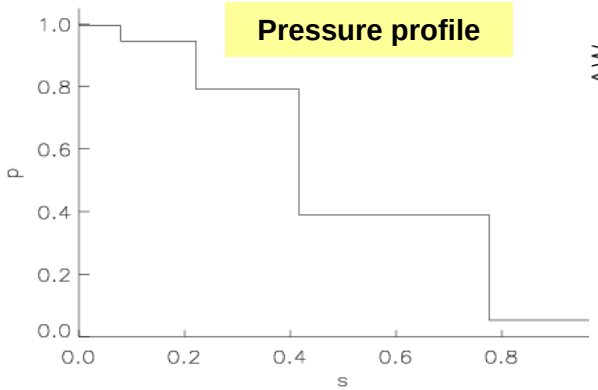

with Fourier resolution, β ≈ 4% case

poloidal resolution $0 \le m \le M$

toroidal resolution $-N \le n \le N$

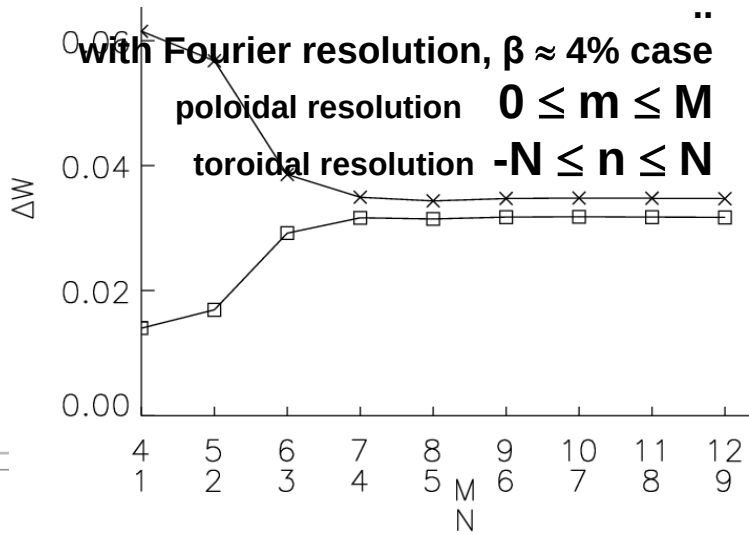

equilibria accurately approximate smooth-pressure *axisymmetric* equilibria

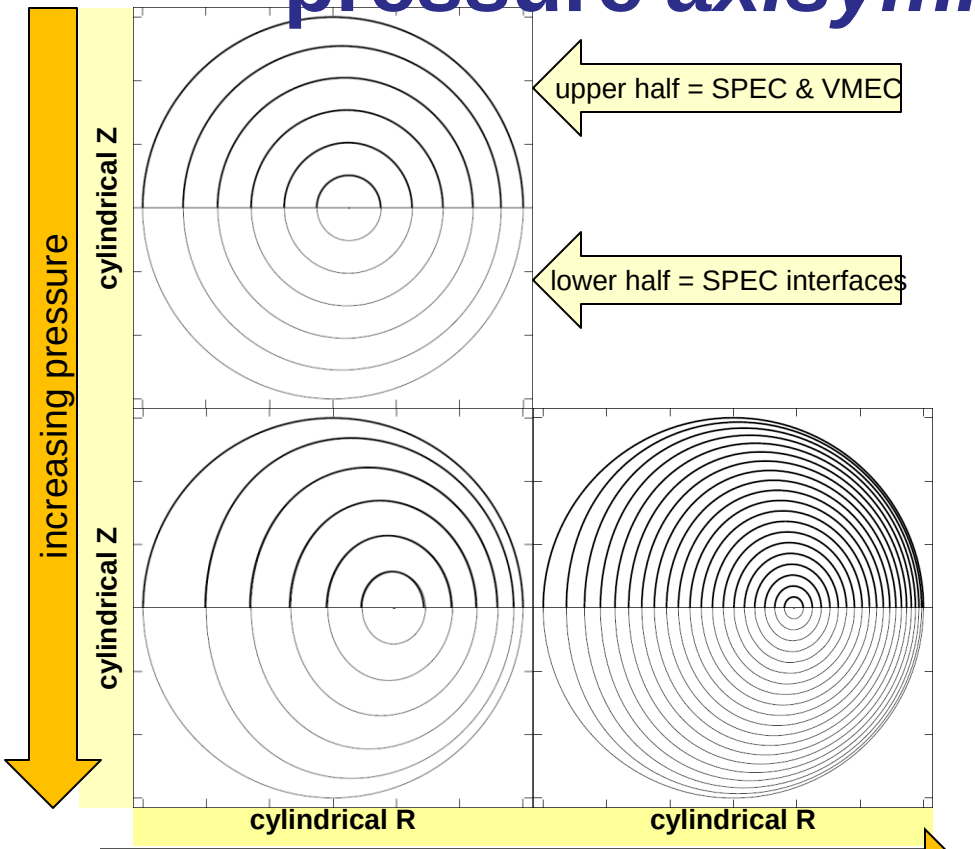

In axisymmetric geometry
- fields have family of nested flux surfaces,
- Equilibria with smooth profiles exist
- Approximation improves with # interfaces
- magnetic axis converges with resolution

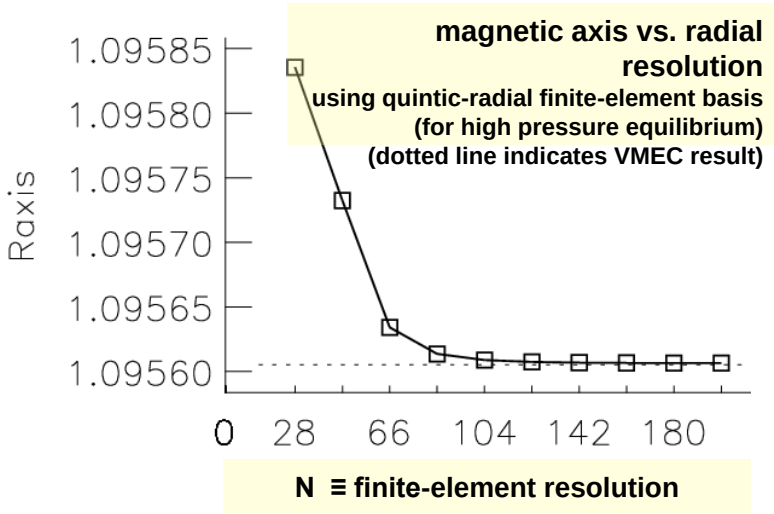

increasing pressure resolution ≡ number of interfaces

stepped-profile approximation to smooth profile

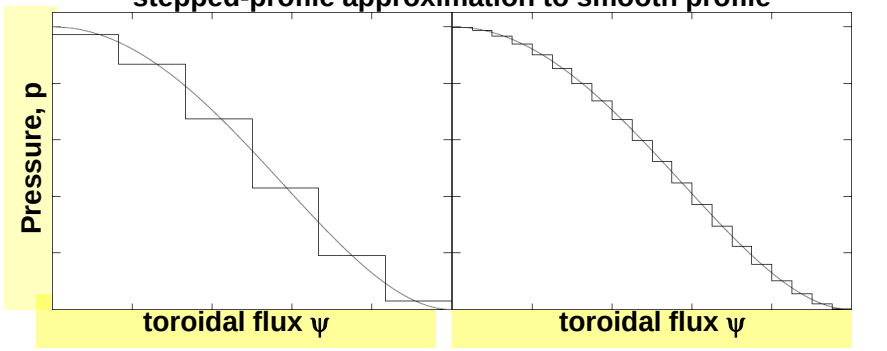

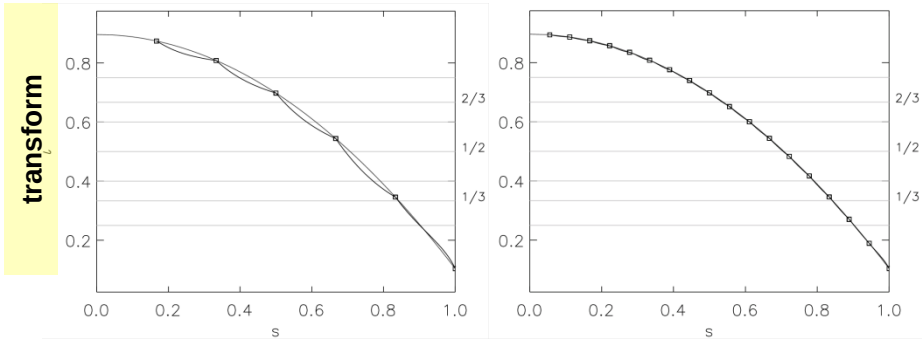

1st variation ⇒"relaxed" equilibria

Energy Functional *W*: $W = \sum_{i=1}^{N} \left(U_i - \lambda_i / 2 H_i - \upsilon_i M_i \right)$

Setting $\delta W = 0$ yields:

P_i : $\quad \nabla \times \mathbf{B} = \lambda_i \mathbf{B}$

$\quad P_i = \text{constant}$

I_i : $\quad \mathbf{B} \cdot \mathbf{n} = 0$

$\quad [[P_i + B^2/(2\mu_0)]] = 0$

V : $\quad \nabla \times \mathbf{B} = 0$

$\quad \nabla \cdot \mathbf{B} = 0$

W : $\quad \mathbf{B} \cdot \mathbf{n} = 0$

n = unit normal to interfaces *I*, wall *W*

$[[x]] = x_{i+1} - x_i$

Poloidal flux Ψ^{pol}, toroidal flux Ψ^{t} constant during relaxation:

P_i : $\quad \Psi_{P_i}{}^{t} = \text{constant}$

V : $\quad \Psi_V{}^{t} = \text{constant}, \quad \Psi_V{}^{pol} = \text{constant}$